This is the Accepted Manuscript version of an article published by Elsevier in the journal *Sustainable Cities and Society* in 2024, which is available at:
https://doi.org/10.1016/j.scs.2024.105862
Cite as: Fan Z, Biljecki F (2024): Nighttime Street View Imagery: A new perspective for sensing urban lighting landscape. *Sustainable Cities and Society*, 116: 105862.

Nighttime Street View Imagery: A New Perspective for Sensing Urban Lighting Landscape

Zicheng Fan[a], Filip Biljecki[a,b,*]

[a]*Department of Architecture, National University of Singapore, Singapore,*
[b]*Department of Real Estate, National University of Singapore, Singapore,*

Abstract

Urban lighting reflects nocturnal activities and it is traditionally observed using Nighttime Lights (NTL) satellite imagery. Few studies systematically measure the nightscape from a human perspective. This study brings a new paradigm — urban lighting sensing via Nighttime Street View Imagery (SVI). The paradigm draws on the accomplishments of (daytime) SVI and gives attention to its ignored nighttime counterpart. We put forward this idea by manually collecting 2,831 nighttime SVIs across various urban functional areas in Singapore. We investigated their values by developing a use case for clustering nighttime lighting patterns. To mitigate the scarcity of nighttime SVI, deep learning regression models were trained to predict nighttime brightness based on corresponding daytime SVIs obtained from widely available sources. The results were compared with brightness data derived from satellite imagery, to affirm the novelty and uniqueness of nighttime SVI. As a result, there are 7 lighting patterns within the collected nighttime SVI, distinct in lighted spot features and total brightness. The identified patterns effectively characterize different urban function scenarios. The best trained brightness prediction model performs well in revealing the city-scale lighting landscape. The SVI-predicted brightness shows a distribution similar to the brightness from satellite imagery and complements it in urban areas with complex vertical lighting structures. This study demonstrates the potential of nighttime SVI as a valuable data source for mapping urban lighting and activities, offering advantages over satellite data. The proposed paradigm contributes significantly to cross-modal information mining in urban studies and has potential applications in scenarios such as light pollution mitigation and crime prevention.

*Corresponding author

© 2024, Elsevier. Licensed under the Creative Commons Attribution-NonCommercial-NoDerivatives 4.0 International (http://creativecommons.org/licenses/by-nc-nd/4.0/)

Keywords:
Social Sensing, Urban Lighting, GeoAI, Urban Analytics, Urban Infrastructure, Urban Informatics

1. Introduction

Thanks to the natural connection among light, human visual senses, and behaviors, artificial lights serve as intuitive instruments to sense the nocturnal human activities. Nighttime Lights (NTL) satellite imagery is the commonly used data reflecting artificial lights, specifically for urban light sources, fishing activities, and oil and gas burning on the Earth's surface (NASA, 2021; Zhang et al., 2022). The typical use cases of NTL data include monitoring urban sprawl (Yang et al., 2020; Duque et al., 2019), economic activities (Mellander et al., 2015; Xu et al., 2021; Zhang et al., 2024), and population growth (Wang et al., 2020; Yu et al., 2019). While NTL data has been applied extensively, there are also significant limitations of this data in reflecting the lighting information. Common problems with NTL data include limited availability of high-resolution sources (Zheng et al., 2023; Zhao et al., 2019), imaging issues such as the blooming effect and the presence of saturated pixels (Zhao et al., 2018; Hu et al., 2019), and the scale effect in modeling geographical phenomenon (Zheng et al., 2023). Due to these challenges, while NTL data is often considered an effective proxy for urban vitality or economic activity at a large spatial scale (Xu et al., 2021; Hu et al., 2024), it remains difficult to use NTL data for precise observation and interpretation of the interaction between urban lighting and activity characteristics at finer levels of detail.

Another limitation is the mismatch between the human perceived urban lighting and the lighting information sensed from satellite level. It is usually less effective to apply NTL data in analyzing the lighting conditions of street-level scenarios, such as in assessing road accident risk (Fotios and Gibbons, 2018), investigating safety perception (Welsh et al., 2022), or understanding the impact of lighting trespass on buildings and human health (Cho et al., 2015; Ntarara et al., 2022). These studies are closely related to the lighting in the urban vertical dimension, from building facades or streetlamps, and require a human perspective for perception (Jackett and Frith, 2013; Rahm et al., 2021; Xu et al., 2018; Sung, 2022). However, limited to the top-to-down imaging method, it is insufficient for NTL data to reveal the diverse urban lighting landscape in urban vertical dimension, leaving significant gaps in the related fields. Beyond NTL data, some studies have employed field measurements (Pan and Du, 2021) and numerical modeling

(Tong et al., 2023) to understand how the vertical dimension of a city is illuminated. Yet, these approaches often suffer from scalability issues due to the limited sampling points and the considerable workload for comprehensive modeling. Consequently, while these methods provide valuable insights, their application remains restricted.

In recent years, Street View Imagery (SVI) data has dramatically expanded our horizons in perceiving urban built environments (Biljecki and Ito, 2021). The unique perspective and method provided by SVI are expected to bring new opportunities in sensing urban lighting. Specifically, advantages of SVI data include the high coverage for urban space on a global scale (Goel et al., 2018), relatively low cost in collection and utilization (Kang et al., 2020; He and Li, 2021), and a flexible, human-centered perspective for environmental observation (Zhang et al., 2019; Biljecki and Ito, 2021). These features make SVI a comparable tool to satellite imagery for urban analytics but with a more detailed, street-level focus. Moreover, with the technological advancements in deep learning and computer vision (CV), researchers are able to translate street view features into other forms of urban information and explore the hidden knowledge embedded in pixels (Ibrahim et al., 2020). This has further expanded SVI's potential applications. Some typical uses of SVI data include identifying specific street and building elements or spatial attributes (Ki and Lee, 2021; Sharifi Noorian et al., 2020; Ao, 2019), evaluating and classifying urban scenes (Aravena Pelizari et al., 2021; Ito and Biljecki, 2021), and geo-localization and reconstructing of 3D street elements.(Pang and Biljecki, 2022; Ning et al., 2022; Cheng et al., 2018). Given these unique features and wide use cases, it is nature to associate SVI with the potential application in sensing street-level lighting landscape during nighttime.

However, in a stark contrast with satellite imagery, which is captured at any time and condition, SVI data is almost exclusively acquired during daytime (Lauko et al., 2020; Hou et al., 2024). The nighttime SVI, which can represent the city life in contrasting lighting conditions and time periods at street level, is almost nonexisting in major commercial or crowdsourced SVI sources. Compared to taking images during the daytime, capturing stable images in low-illumination environments at nighttime presents more technical difficulties and higher costs (Shi et al., 2018), and often less information can be obtained and recognized. Some studies focused on nighttime lighting may capture a small number of nighttime SVI to describe specific lighting characteristics of a scene (Pan and Du, 2021; Lin et al., 2023). However, the brightness information revealed by the images themselves, such as the distribution of light sources and lighting intensity, has seldom been the subject of analysis in the body of knowledge. In a rare and recent case, a small

quantity of nighttime SVI was collected to evaluate visitors' sense of safety in city parks (Lis et al., 2023). However, the study was limited by highly homogeneous scenes. The potential of nighttime SVI in mapping wider urban lighting landscape have yet to be explored.

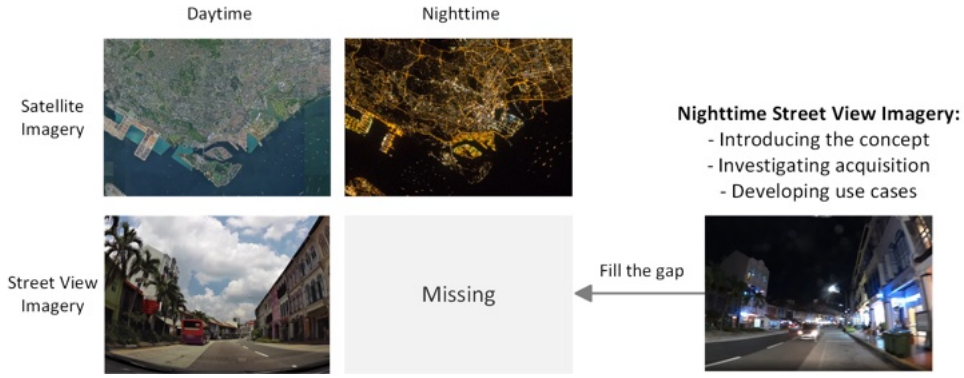

Figure 1: The widely used types of urban imagery and a new instance we propose in this paper. Daytime and nighttime satellite images (top) and street view imagery (SVI), which is almost always collected during daytime (bottom left), have been used for myriads of purposes. In this research, we fill this gap and investigate whether there is value in giving attention to an untapped means of urban sensing – nighttime SVI, conducting a comprehensive study on two aspects: their acquisition and use cases, understanding urban dynamics they can reveal and their added value with respect to the traditionally used urban data sources and imagery. Sources of imagery: Mapillary (daytime SVI); Google Maps (daytime satellite imagery); NASA (nighttime satellite imagery).

Given the overlooked significance of nighttime SVI and its potential in street-level perception, the study explores the usability of nighttime SVI and introduces a novel urban sensing paradigm to apply nighttime SVI in investigating the nighttime lighting landscape from a human-centered perspective. A conceptual framework of the study is illustrated in Figure 1. The new paradigm is founded on two bases. Firstly, the nighttime SVI should not be expected to be analyzed in the same way as daytime SVI (i.e. segmentation, mapping objects) and used for the same use cases. Instead, the brightness and lighting information embedded in the image, as unique indicators of nighttime urban environments, can be extracted from nighttime SVI and be investigated in a similar fashion as NTL satellite imagery. Secondly, considering daytime and nighttime SVI as paired reflections of urban environment at different periods, the street furniture, plants, and building components in a daytime SVI are assumed to indicate the potential activities and brightness information of the corresponding nighttime scenario. In this way, the existing daytime SVI can help address the data scarcity problem and aid in en-

hancing the utilizing of nighttime SVI in urban research. The new paradigm is expected to alleviate the limitations of NTL satellite imagery in measuring the urban lighting landscape and provide appropriate research tools to investigate street-level lighting conditions, serving various research fields such as crime prevention, urban disaster mitigation, and energy management.

Based on the discussion above, the main research question we seek to answer in this paper is:

> Can street-level imagery taken during nighttime be a novel urban dataset useful for urban analytics and to what extent can it be used?

Stemming from it, there are four sub-questions this study aims to answer:

Q1: How can we efficiently collect nighttime SVI data?

Q2: Can any significant nighttime lighting patterns be detected from nighttime SVIs and how are they related to different urban functional scenarios?

Q3: To what extent can we predict the brightness of a nighttime urban scenario based on its corresponding daytime SVI?

Q4: How different are the urban lighting patterns sensed from street level and from satellite imagery, and what is the potential benefit of learning the street-level brightness besides its satellite counterpart?

Taking Singapore as the study area, the research is divided into four stages, corresponding to the sub-questions. Firstly, we manually collect nighttime panoramic imagery across various urban functional areas in Singapore and offer insights about it. Together with the matched daytime counterparts from Google Street View, we aim to create a novel day-night paired SVI dataset as the basis of sensing urban lighting in this study. Secondly, we identify the homogeneous lighting patterns with clustering methods from the collected images. Our goal is to explore a quantitative and efficient way to represent the lighting information embedded in nighttime SVIs, and enable a multi-area investigation of the association between lighting conditions and urban functions. Thirdly, we develop a Deep Convolutional Neural Network (DCNN) model to predict the overall brightness of the nighttime scenarios based on daytime SVIs. The aim is to gain a scalable way to learn the street-level lighting landscape at city scale, while also addressing the scarcity of nighttime imagery by leveraging the more readily available daytime SVIs. Fourthly, we compare the SVI predicted brightness and the brightness

derived from satellite imagery. The aim is to gain further understanding of street-level lighting landscape and to learn the association of this novel dataset we give attention to with the traditionally used instance collected from satellites.

2. Related work

2.1. Sensing Nighttime Human Activity via Lights

Since the 19th century, the availability of artificial lights have been associated with wealth and modern society (Green et al., 2015; Levin et al., 2020). Buildings and roads illuminated by lights suggest nocturnal activities, and the changes in nighttime lighting landscapes are proved to reflect deep changes in human activity patterns (Henderson et al., 2012). The following section introduces the observation of urban lighting from two perspectives: the satellite level and the street level.

2.1.1. Nighttime Lights Observed from Satellite Platforms

The Nighttime Lights (NTL) satellite imagery has been widely applied to observe urban lighting from large spatial-temporal scales (Zheng et al., 2023). This approach has various application scenarios, notably in assessing economic vibrancy (Mellander et al., 2015; Xu et al., 2021), mapping population densities (Wang et al., 2020; Yu et al., 2019), extracting urban functional areas (Hu et al., 2024), monitoring urban sprawl (Yang et al., 2020; Duque et al., 2019), and energy consumption modeling (Wang and Lu, 2021; Xie and Weng, 2016). The intensity of light in these images often associates with urbanization levels(Zhang and Li, 2018), economic activity density (Wang and Sun, 2022), and light pollution extent (Xiao et al., 2020; Ritonja et al., 2020).

Despite the advances, NTL satellite imagery faces challenges in accurately depicting urban lighting conditions and urban activity and function characteristics at a detailed level. Key concerns include data availability and scale effect. In terms of availability, the primary data sources for NTL studies include DMSP-OLS, Suomi-NPP VIIRS, and NOAA-20 VIIRS, which have relatively low spatial resolutions (15 arcsec or 30 arcsec) but available to free access (Zheng et al., 2023; Levin et al., 2020). Issues such as blooming effect and pixel saturation often compromise the reliability of these NTL data in mapping built environment details or human activities (Zhao et al., 2018; Hu et al., 2019). Recent developments in medium and high-resolution NTL products, such as Luojia-1 (130m), Lookup-1 (60m), and SDGSAT-1 (10m for Pan, 40m for RGB) present new possibilities in NTL studies. However, the accessibility and spatial coverage of these medium or

high-resolution NTL products are often restricted, as they are primarily commercial data or data available only to certain organizations.

Another prominent issue in NTL-based research is the scale effect, where the correlation between light and socio-economic indicators can vary significantly with different analysis scales or image resolutions (Bennett and Smith, 2017; Guo et al., 2024; Zheng et al., 2023). This variability introduces challenges in accurately mapping and modeling urban socio-economic indicators based on NTL. Though there are suggestions to combine NTL sources at different resolutions to enhance the robustness (Zheng et al., 2023), the choices are limited to combine low-resolution and high-resolution NTL data, which can also suffer from the availability of NTL data. There is a lack of another data source similarly reflecting the nighttime lighting features, beyond satellite platforms, and one that can be less rigid and available across different scales.

2.1.2. Nighttime Lights Sensed at Street Level

From a human-centered perspective, urban lighting is more commonly sensed at street level. The association between street-level lighting and nocturnal activity and behavior receive significant attention. Proper lighting conditions are recognized as a positive factor in boosting street activities (Zhang et al., 2021). Typically, lights are considered a deterrent to criminal behavior (Painter and Farrington, 1999; Cornish and Clarke, 2014), and help expand pedestrians' field of vision and reduce fear (Kaplan and Chalfin, 2022). In an experiment based in New York City, Chalfin et al. (2022) demonstrated that neighborhoods that were temporarily allocated more street lamps had a significant decrease in nocturnal outdoor crimes. Enhanced street lighting is a possible mechanism to intervene and reduce crime. Additionally, street-level lights play a crucial role in facilitating urban traffic, specifically in reducing the frequency and severity of accidents (Yannis et al., 2013; Wanvik, 2009; Walker and Roberts, 1976). Lights also serve as key components in shaping and highlighting urban landmarks and public space in the urban design context (Pan and Du, 2021; Alves, 2007).

Despite the benefits, street-level lighting can also bring negative social outcomes. Excessive light exposure in the nighttime is reported to interfere with circadian rhythms (Vallée et al., 2020), reduce melatonin secretion (Chen et al., 2020), disrupt sleep (Zielinska-Dabkowska et al., 2023), and strain the visual system (Lunn et al., 2017). Light trespass is a typical form of indoor light pollution related to health risks, and it is often caused by excessive light emission from building facades, billboard, street lamps (Chen et al., 2020; Sung, 2022), featured in vertical dimension of street-level lighting. Overall, there are close and com-

plex associations between street-level lighting and nocturnal activities, where the benefits of lighting must be carefully weighed against its potential health and environmental impacts.

Various methods have been employed to measure street-level lighting conditions. Self-reported questionnaires and mechanical statistics on street lamps are common approaches in crime or safety-related studies (Kaplan and Chalfin, 2022; Chalfin et al., 2022). However, these methods often yield only a vague understanding of lighting conditions and are somewhat subjective. In contrast, in the health field, field measurements with light meters and numerical modeling are typical methods for precisely assessing the lighting environment of small-scale outdoor spaces (Tong et al., 2023; Chen et al., 2020). Nevertheless, these methods are also limited by the number of sampling points and the workload involved in modeling, making them less scalable. The NTL satellite imagery has been applied as proxy of street-level lighting to examine its association with health issues on a large spatial scale (Helbich et al., 2020; Xiao et al., 2020; Ritonja et al., 2020). However, a significant conflict arises as NTL satellite imagery primarily captures upward light emissions from a top-down perspective, while light from many nocturnal urban activities is emitted horizontally and from the vertical dimension of the urban environment. As a result, NTL data may be insufficient to represent lighting environment with diverse vertical lighting structure and in human-centered scenarios.

In summary, due to the limitations of different technologies, it is considered inadequate to only rely on a single technique in the lighting measurement (Wang et al., 2023). A combined application of different techniques, incorporating both vertical and horizontal perspectives of light emission can be significantly more effective. Additionally, there is a pressing need to explore new data sources and methods capable of capturing the street-level lighting environment with high detail and extensive spatial coverage.

2.2. Sensing Urban Lighting Landscape via SVI

Addressing these challenges, Street View Imagery (SVI) has emerged as a valuable resource in urban research, offering new opportunities to sense urban environments at a finer scale. SVI provides a unique perspective by capturing the streetscape from a human-centered viewpoint, thus enabling a potentially more comprehensive understanding of urban lighting and its interaction with the built environment. The following section introduces the general data sources, applications and limitations of SVI, and its potential in lighting sensing.

2.2.1. SVI Sources, Applications and Limitations

There are multiple SVI sources, spanning commercial and crowdsourced types. In terms of commercial services, Google Street View is the largest such provider, covering more than 90 countries and regions (Biljecki and Ito, 2021); while other map companies, such as Baidu Maps and Tencent Maps, provide similar regional services (Kang et al., 2020). Besides, a few crowdsourced SVI services have emerged in recent years, such as Mapillary and KartaView, where SVI, as an emerging form of Volunteered Geographic Information (VGI), are provided by contributors around the world and uploaded for free use (Hou and Biljecki, 2022). Serving research demands in Computer Vision (CV) and autonomous driving fields, open street view datasets such as Cityscapes (Cordts et al., 2016), ADE20K (Zhou et al., 2019), CAMVID (Brostow et al., 2009) have also been widely used.

The application of SVI in current urban research is widespread, benefit from the enrichment of the SVI sources, and the rapid development of deep learning. Many scholars have systematically reviewed the common deep learning models for SVI and their specific usage scenarios in urban analytics and research (Ibrahim et al., 2020; Kang et al., 2020; Biljecki and Ito, 2021; He and Li, 2021; Zhang et al., 2023a). From a model perspective, the Convolutional Neural Network (CNN) is a class of deep learning models and structures widely used in SVI analysis. CNN functions by constructing and differentiating multiple hidden layers in the neural network, to extract digital features that may or may not be recognized by human eyes from images (Guo et al., 2016; LeCun et al., 2015). CNN and its derived models can be applied in specific CV tasks such as image classification, semantic segmentation, object tracking, activity perception and scene understanding. These tasks further contribute to urban analysis scenarios of spatial infrastructure, transportation, greening, health, and socio-economic activities. In addition to CNN, other common deep learning models for SVI include the Generative Adversarial Networks (GAN), used to achieve style transfer (Jiang et al., 2021) and image restoration (Liu et al., 2021); Graph Neural Networks (GNN), for linking SVI with street scenes and associated geographic information (Zhang et al., 2023b).

Though abundant sources and wide applications, the data availability of SVI in nighttime scenario is a main concern. As poor lighting conditions can amplify the difficulty of capturing SVIs and reduce the information obtained (Shi et al., 2018), both commercial and crowdsourced sources strive to collect SVIs in daytime and in clear and sunny weather. The nighttime SVIs are rarely collected, and are recognized as *noise*, considering its limited usability in almost all of the typical

applications daytime SVIs are routinely used, such as urban form measurement, assessing walkability, and supporting real estate valuations (Woo et al., 2024; Biljecki et al., 2023; He and He, 2023). For example, Google Street View does not collect nighttime SVI data, while KartaView explicitly declines SVI taken at night and during raining, snowing and fog (KartaView, 2020). A recent investigation on crowdsourced SVI datasets across hundreds of cities reveals that only about 3.1% of images in Mapillary are taken during nighttime (Hou et al., 2024).

2.2.2. Potential of SVI in Sensing Nighttime Scenarios

Nevertheless, there are valid reasons to collect, explore and utilize the nighttime SVI, and give more attention to this latent type of urban data and perspective of SVI. As a direct information holder of urban nighttime environment, a few practices have demonstrated the value of the data. In automotive industry for example, nighttime SVIs are applied to improve the robustness of autonomous driving system in poorly illuminated environments. A small number of day-night paired SVI datasets have been collected and released openly for deep learning tasks, such as TOKYO 7-24 (Torii et al., 2015) and BDD100K dataset (Yu et al., 2020). However, coordinates and other meta data are generally missing in the datasets, which limits their application in urban studies, and makes independent and systematic collection of nighttime SVI as a necessary choice. Furthermore, when compared to NTL data, which predominantly offers a top-down view of the urban nighttime landscape, nighttime SVI may hold a distinct advantage. While not given attention hitherto, it is expected that the nighttime SVI can offer a more accurate representation of light source distribution at street level and furnishes a more versatile and granular perspective for portraying the nighttime urban environment and activities.

In addition, one growing trend in recent SVI research is that, SVI has been proved not merely a reflection of urban visual feature, but also a useful medium for learning cross-modal physical features of urban space, which help solve the data scarcity problems of nighttime SVI. The type, number, size, and location of various street features represented in SVI may reflect the properties of sound, heat, and light associated with the urban environment. For example, Zhao et al. (2023) develop a a machine-learning framework for portraying large-area urban soundscapes using SVI features, without ground measurements. Similarly, Ignatius et al. (2022) explore the potential of SVI in assisting Local Climate Zone (LCZ) classification, and in enhancing the understanding of Urban Heat Island (UHI) in high-density city. Additionally, there have been innovative applications of GAN models alongside SVI for the day-night style conversion of urban land-

scapes (Zhu et al., 2020; Anoosheh et al., 2019; Jiang et al., 2021). The cross-modal adaptability of SVI presents a promising challenge in utilizing daytime SVI to investigate nighttime urban environments. Liu et al. (2024) discussed the potential of generating nighttime SVI with GAN models for urban scene auditing and conducted positive explorations. However, the day-night images collected for model training in their work are from homogeneous scenes and in limited perspectives, which is not applicable for mapping urban-scale, street-level lighting conditions. In our work, as the paper will describe later, we collect real nighttime SVI using own data collection.

In conclusion, both collecting and utilizing nighttime SVI itself, and using daytime SVI as a medium to represent nighttime scene attributes, hold significant potential in urban sensing research. Focusing on the most fundamental information reflected by nighttime SVI, brightness, this study integrates these two approaches to propose a novel paradigm for nighttime urban lighting sensing. The details are elaborated in the following sections.

3. Methods

An overall research framework is illustrated in Figure 2, corresponding to the research questions described in the Introduction. Divided into four stages, the main tasks include: firstly, a large-scale collection of day-night paired SVI across multiple scenes; secondly, nighttime lighting landscape analysis with clustering method; thirdly, nighttime brightness estimation based on daytime SVI; fourthly, interpretative analysis of the potential connections between SVI predicted brightness, satellite derived brightness. and other urban activity data.

3.1. Collection of Day - Night SVI data

The research first collected day - night paired SVIs in Singapore to investigate the nighttime urban lighting characteristics. Sources of SVIs include: (1) nighttime panoramic SVIs manually collected with a GoPro Max 360 camera mounted on a bicycle, and (2) daytime panoramic SVIs collected through the Google Street View API.

The nighttime panoramic SVIs were systematically collected from five built-up districts in the city-state, namely the industrial park area in Tuas, the high-rise residential area in Pioneer and Jurong, the low-rise residential area in Holland Village, the university campus, communities, and highway areas in Clementi, and the low-rise and high rise commercial areas in the Central Area of Singapore. Though limited image numbers due to workload constraints, the collection encompasses

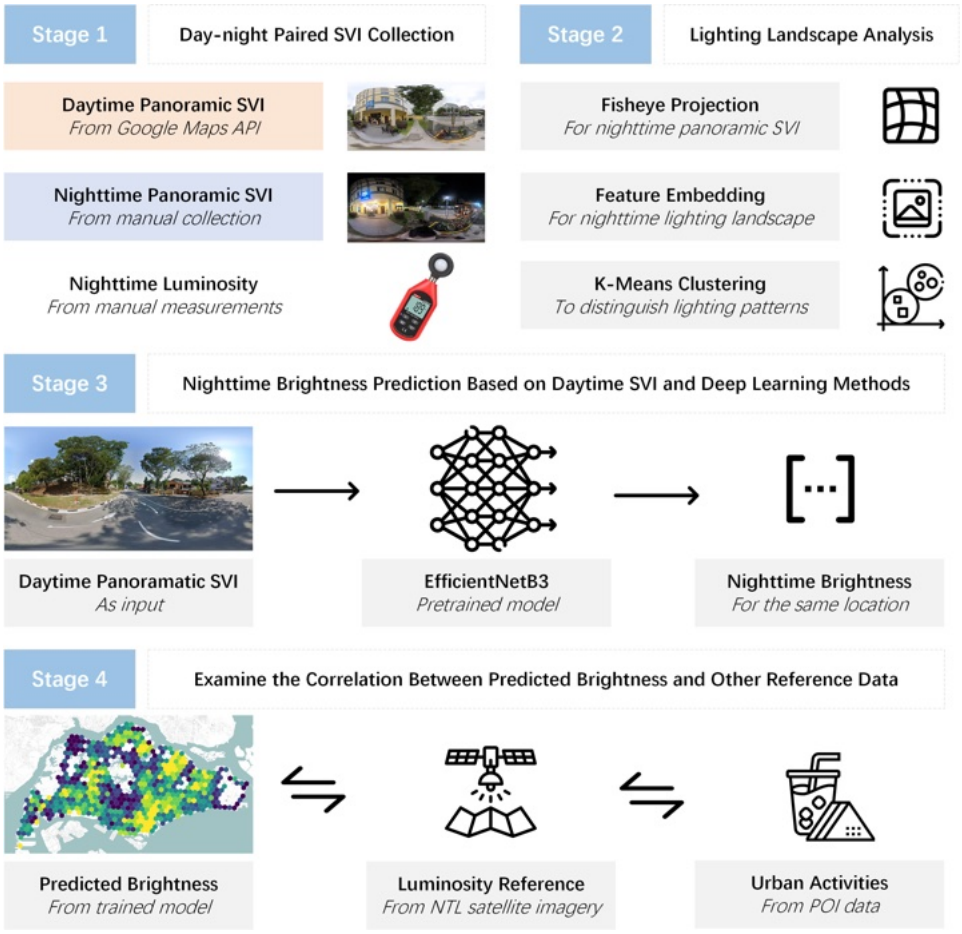

Figure 2: Four steps of the research framework. Sources of imagery: Google Street View, Flaticon.

a diverse range of urban forms and functions, spanning across typical community types in Singapore, making it broadly representative. Besides SVIs, a luminance meter is used to measure and record the brightness value of the corresponding street scenarios for data validation and reference. Figure 3 illustrates both the image collection points and the device measured luminosity value at the same location. A wide variety of urban functional scenarios were captured in the data collection.

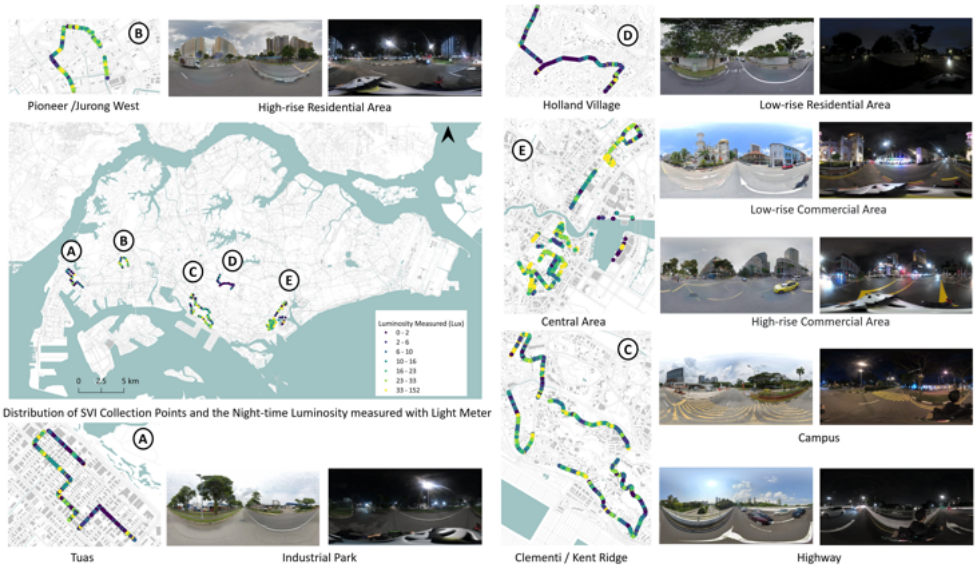

Figure 3: Spatial distribution of SVI collection points, luminosity values (with unit of lux) measured at the collection points, and sample panoramas in local areas. Source of the basemap: OpenStreetMap. Sources of SVI: Google Street View (daytime SVI); our manual collection (nighttime SVI).

The nighttime panoramic SVIs were captured while cycling at a constant speed using a GoPro Max 360 camera, mounted at a height of 1.7 meters above the ground. The images were consistently collected from 20:00 to 23:00 after sunset, and spanning from August to November in 2023. This later timing for collecting images was chosen to minimize the influence of extra sky light sources on the SVIs while maximizing the lighting information from on-street urban activities. Following the best practice introduced by Mapillary, a popular platform for crowdsourced SVIs, the images were first shot as time lapse videos at an interval of 0.5 seconds and 5.6K resolution, and then single images were extracted with time stamp and location information. The luminance meter was placed horizon-

tally upward during measurements, and the luminosity values were matched with the collected images according to their nearest distance on the timelines. Using the coordinates of nighttime panoramic SVIs, the nearest daytime panoramic SVIs were searched and collected from Google Street View.

While collecting SVI data, we identified several potential sources of bias. For instance, the camera shake while cycling may cause blurry images, and sudden changes in lighting conditions could result in overexposure. Additionally, urban canyons might affect GPS positioning accuracy and amplify the positional discrepancies between the collected nighttime SVI and the searched daytime images. To mitigate the impact of these biases, we manually inspected and cleaned the collected data. A total of 2831 pairs of well-matched day-night SVIs were selected for subsequent analysis, including nighttime lighting landscape investigation and the training for a brightness prediction model. Another 50 689 daytime SVIs in Singapore, across 2015–2023, were collected to scale the trained model to predict the nighttime brightness across the city.

3.2. Nighttime Lighting Landscape Analysis

The urban nighttime landscapes are essentially composed of objects illuminated and visible at night. The research explores the consistency patterns reflected in nighttime lighting landscape, by analyzing the size and distribution patterns of various lighted spots in nighttime SVIs and the total luminosity of the scene.

3.2.1. Lighted Spot Detection

The first step is to extract the significant lighted spots from nighttime SVIs. As shown in Figure 4, a series of CV methods were applied, including the image projection transformation, pixel-level brightness calculation, and lighted spot contour extraction. Specifically, the research first attempted to transform the panoramic images from an equidistant cylindrical view into a top-down fisheye view. The nighttime panoramic SVIs were initially produced with an equidistant cylindrical projection via the GoPro Max camera, and the projection tended to overly emphasize ground features at lower elevations while compressing and distorting elements such as buildings, trees, and streetlights at higher elevation. The latter plays a crucial role in constituting nighttime lighted spots. By transforming the panoramic SVIs to top-to-down fisheye format, the proportions of various built environment elements were balanced in the images.

On this basis, the study attempted to convert the color mode of the SVIs from RGB to grayscale and calculate the brightness of each pixel. The pixel-based

brightness formula is given by:

$$\text{Pixel based Brightness} = 0.299R + 0.587G + 0.114B$$

where R represents the red channel value of the pixel, G represents the green channel value of the pixel, B represents the blue channel value of the pixel. Then, the method extracted the continuous contour lines and areas whose pixel-level brightness is significantly higher than the surroundings as lighted spots. The developed procedure has also uniformly removed the ground portion from the images, because it tended to be identified as lighted spots in the algorithm, while introducing significant noise due to its color and material variance in different lighting scenario.

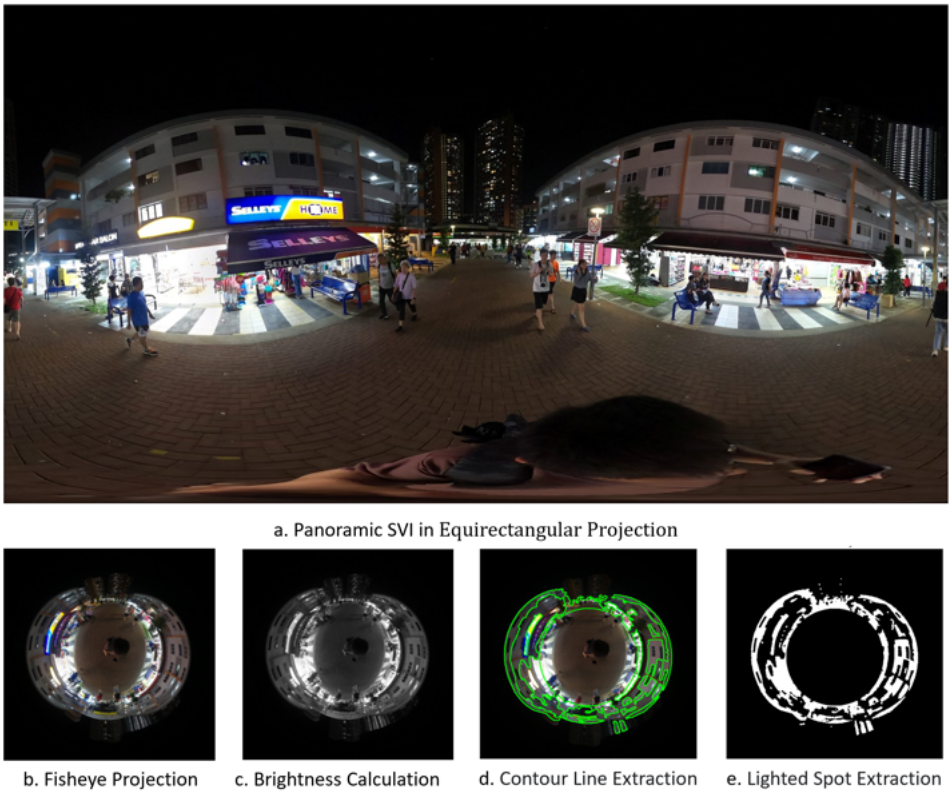

Figure 4: Workflow to extract lighted spot features from nighttime SVI. The panoramas are transformed into a top-down fisheye view with the pixel-level brightness calculated. Continuous pixels that are significantly brighter than the surroundings are extracted as 'lighted spots'.

3.2.2. K-means Clustering

It was assumed that the urban lighting landscape can be described via a series of fixed and generic lighting patterns behind the diverse nighttime lighting scenarios. The research utilized the *k*-means clustering method(Hartigan and Wong, 1979) to identify the generic lighting patterns, based on the similarities and differences in the features of nighttime SVIs and the luminance meter records (Wang and Biljecki, 2022). Each nighttime SVI collection point served as an observation, and the lighted spots characteristics within the images, including the total area of lighted spots, and average distance of lighted spots to the image centroid, together with total luminosity measured from light meter, were calculated to represent the overall features of the corresponding nighttime lighting scenarios. The study employed the silhouette method (Rousseeuw, 1987) to determine the optimal number of clusters, denoted as K. One-way Analysis of variance (ANOVA) and Tukey's honest significant difference (HSD) post-hoc test were applied to investigate and validate differences between the clustering groups. The clustering results were further compared with the daytime street view elements, road levels, and urban function labels corresponding to the respective street scenes in frequency distribution. The aim was to interpret the association between nighttime lighting conditions and daytime street view elements, as well as various urban activities and functions.

3.3. Nighttime Street Brightness Prediction

After the initial exploration of the urban lighting landscape represented by nighttime SVIs and luminance meter records, the study trained a deep learning model to predict the brightness of corresponding nighttime scenes using daytime SVIs. By further scaling the model to cover daytime SVIs across Singapore, the research aimed to gain insights into the urban-scale nighttime lighting landscape characteristics.

3.3.1. Model Training

Building upon pre-trained image classification models, the research employed the transfer learning approach to train a regression model to predict nighttime street-level brightness based on daytime SVIs. TensorFlow was used as the training platform, and various mainstream architectures were explored and compared, including EfficientNet (Tan and Le, 2020), Vision Transformer (ViT) (Dosovitskiy et al., 2021), VGG16 (Simonyan and Zisserman, 2015), and ResNet50V2 (He et al., 2015, 2016). Among them, VGG16 and ResNet50v2 are well-established deep convolutional neural networks, both excelling in image classification tasks.

EfficientNet and ViT represent modern advancements, with EfficientNet balancing accuracy and efficiency through systematic scaling, and ViT leveraging the transformer architecture to capture long-range dependencies, performing exceptionally well on large-scale datasets. These selected models were all pre-trained on the ImageNet image classification dataset (Deng et al., 2009). By retaining the pre-trained model weights, removing the classification head, and introducing new dense layers and activation layers, the study adapted the pre-trained models for regression tasks.

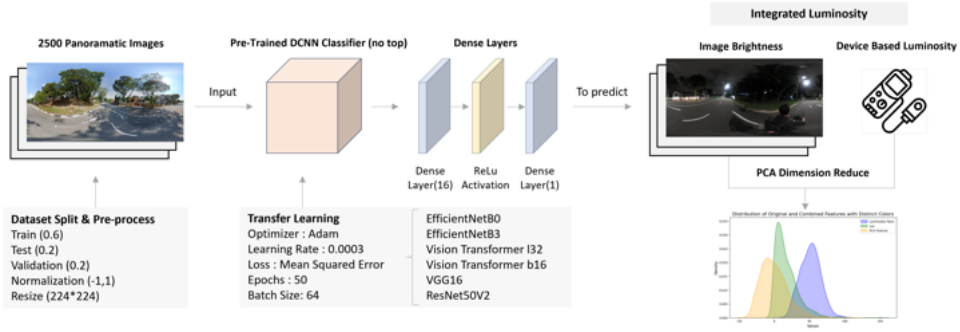

Figure 5: Workflow for model training.The daytime SVIs are the model inputs, and the expected outputs are the brightness of nighttime scenario corresponding to the daytime SVI.

Figure 5 illustrates the model training process. The training of the brightness prediction model relied primarily on 2500 pairs of matched daytime and nighttime SVIs. To efficiently scale the model to cover a large-scale SVI dataset, the study used equidistant cylindrical views of daytime SVIs as model inputs, as it is a common format the daytime SVIs are stored and released. Principal Component Analysis method (PCA) (Wold et al., 1987) was applied to extract a principal component from the device measured luminosity and the brightness calculated from nighttime SVI, as an integrated brightness variable to predict. The aim was to maintain the maximum of brightness characteristics captured in two lighting sensing methods, while eliminating the potential impact of outliers. The dataset was divided into training, testing, and validation sets in a 3:1:1 ratio, with image resizing and pixel value normalization applied consistently. Mean Squared Error (MSE) was the primary metric for monitoring training, supplemented by Mean Absolute Error (MAE) and Root Mean Squared Error (RMSE) for model comparison. Given the relatively small training dataset and the study's broader focus, fine-tuning was limited to basic model hyper-parameters and training strategies. Our focus on hyper-parameter selection was primarily driven by comparing the

performance of different base model architectures. The model architectures served as feature extractors, each incorporating a dense layer with 16 units, ReLU activation, and a final dense layer for regression. More denser layers or larger layer size were avoided due to performance degradation in early tests. Additionally, each model was trained for a maximum of 50 epochs. The learning rate was initially set to 0.0003, with a reduction applied if performance did not improve within 3 epochs, and early stopping was triggered after 10 epochs of no improvement. To validate the performance of deep learning methods, we also fitted traditional regression models such as Ordinary Least Squares (OLS), Random Forest (Breiman, 2001) and XGBoost (Chen and Guestrin, 2016) as baselines. The inputs for these models included segmented street view features extracted from daytime SVIs and the road classes of the image locations, with the same integrated nighttime brightness values from PCA serving as the output.

3.3.2. Further Analysis

We scaled the best trained model to 50 689 daytime SVIs across the entire Singapore, to predict the nighttime brightness of the corresponding scenarios and map the city-scale lighting conditions. With the SVI predicted brightness values, the study investigated its spatial distribution difference and correlation with the urban-scale brightness features obtained from the NTL satellite imagery. Previous study by (Lin et al., 2023) has preliminarily revealed the correlation between illuminance measured on the street-level and Digital Number (DN) from satellite imagery. Our goal is to assess in which areas and in which ways, the two sensing methods and data sources can capture the urban lighting information similarly and differently.

The NTL data was primarily sourced from the Sustainable Development Science Satellite 1 (SDGSAT-1) developed by the Chinese Academy of Sciences (CAS)[1]. The satellite employs glimmer imager with an imaging resolution of 40 m for RGB band and a swath width of 300 km (Guo et al., 2023). The imagery over Singapore was captured on June 29, 2023. There are two additional NTL sources applied in this study, to validate SDGSAT-1's imagery with different resolution and capture time. The additional NTL sources include Luojia-1 NTL imagery from Wuhan University[2] and Visible and Infrared Imaging Suite (VIIRS) Day Night Band (DNB) NTL imagery from Earth Observation Group (EOG)[3]. The

[1] `https://www.sdgsat.ac.cn/`

[2] `http://59.175.109.173:8888/index.html`

[3] `https://eogdata.mines.edu/products/vnl/#monthly`

former was retrieved on September 30 in 2018 with a resolution of 130 m, and the latter was a monthly cloud-free composite from 2023 May with a resolution of 500 m.

The OLS regression model was initially employed to establish a potential linear relationship between predicted brightness and satellite derived brightness. By conducting a local Moran's I analysis on the residuals of the OLS model, the study examined whether there is spatial auto-correlation in the interaction between SVI predicted brightness and satellite derived brightness. If such auto-correlation exists, the spatial-lag regression model was applied to refine their relation, with spatial neighboring effect taken into account. In addition, the study also investigated the correlation between two brightness features and the urban activities features represented by POI counts. The aim was to check whether there is a potential of SVI predicted brightness to map the urban activities distribution, and compared to the satellite derived brightness, if it is possible for the SVI predicted brightness to be a meaningful alternative or a supplement to NTL data derived from satellite imagery.

4. Results

4.1. Lighting Landscape Clustering

4.1.1. K-means Clustering Result

The section details results from k-means clustering analysis, where seven clusters were identified as optimal for a balanced and informative partition of lighting scenarios. As shown in Figure A.15 and Figure A.16 in the appendix, this decision is supported by the mean silhouette scores derived from 50 random experiments conducted for each k value. Although the silhouette score is highest at k=3, we chose k=7 because it achieved the highest silhouette score improvement among all k values greater than 4, allowing us to better capture the diversity of the lighting scenes. Additionally, the one-way ANOVA and the Tukey's HSD test further revealed significant differences in three lighting features between different clustering groups, as shown in Table A.3, A.4, A.5, and A.6. Figure 6 displays the distribution of these seven unique clusters in the feature space. Key differences among the clusters are primarily in the total luminosity of the scene and the area covered by lighted spots. There is an observable trend from Cluster 0 (lower luminosity and smaller lighted spots) to Cluster 2 (higher luminosity and larger lighted spots). In clusters with similar luminosity and spot area, the distance of lighted spots from the image center offers additional differentiation. Cluster 6, for

instance, has lighted spots further from the center, indicating a higher positioning relative to the horizon, while Cluster 1 features the darkest scenes with the smallest and lowest lighted spots.

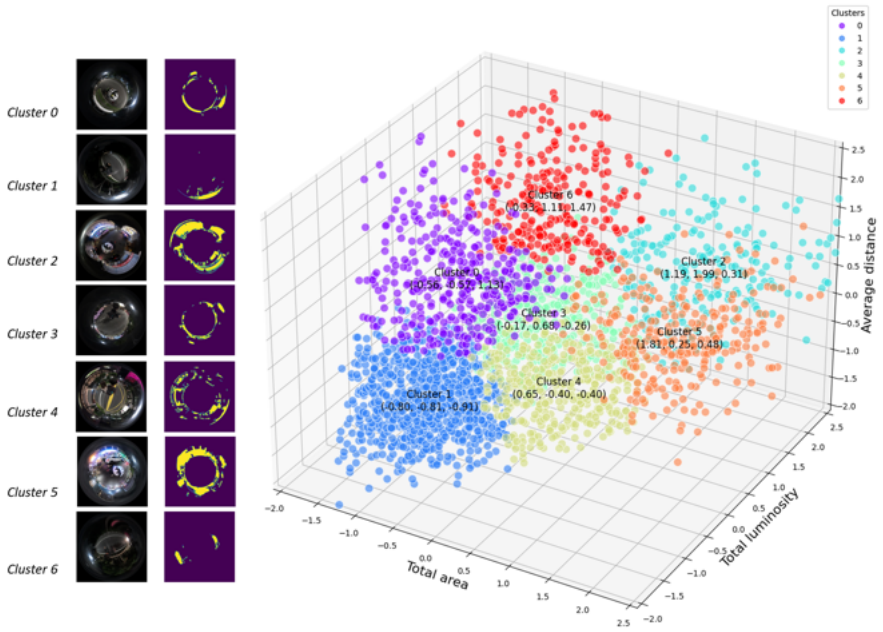

Figure 6: Clustering visualization in 3D feature space.

The study also examines the relationship between nighttime lighting patterns and daytime street view features, along with road levels. As shown in Figure 7, across the clusters, flat elements (such as roads and pavements) and sky elements remain consistent in proportion. However, clusters with brighter and larger lighted spots tend to have more construction features and fewer natural elements. In terms of road levels, brighter clusters (e.g. 2, 3, 4, 5) have a higher presence of secondary roads and fewer residential roads, contrasting with darker clusters (e.g. 0, 1, 6). Notably, there is a consistent varying pattern observed from the night time lighting patterns and the daytime street view and road levels, suggesting that road scenes perceived and functioning differently during the daytime are likely to maintain the difference in nighttime lighting characteristics.

4.1.2. Relation between Lighting Pattern and Functional Scenario

The significance of different lighting clusters can be further analyzed in relation to their real-world locations and functional scenarios. Figure 7 illustrates the

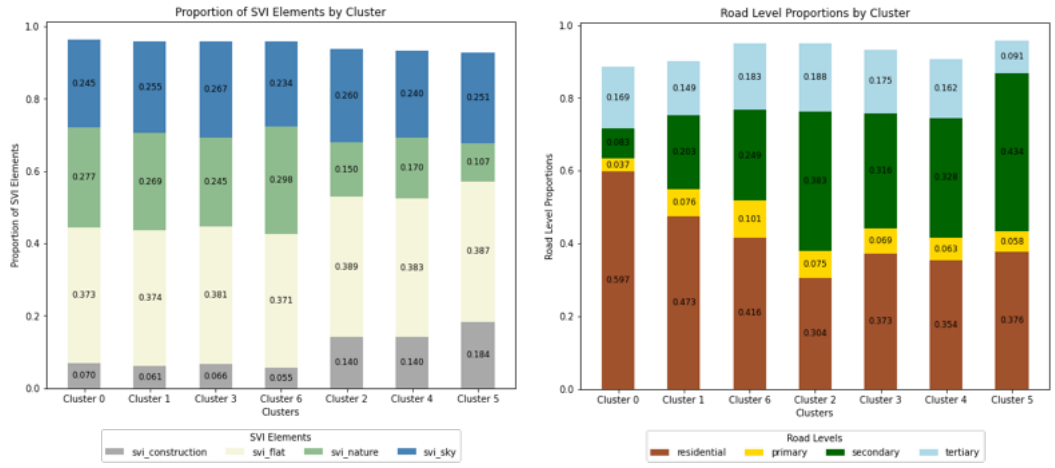

(a) SVI proportion for all clusters.

(b) Road proportion for all clusters.

Figure 7: Cluster average of the street view element proportions and road level proportions.

spatial distribution of different nighttime lighting clusters in local areas of Singapore and measures the conditional frequencies of various lighting patterns in each urban functional scenario. Notably, clusters with higher luminosity and larger spot areas (e.g. 2, 4, 5) are predominantly found in the Central Area of Singapore. Bright and prominently sized light spots in SVIs correspond to storefronts along streets, large billboards, and architectural windows, as well as other facade lighting, indicating significant service and commercial characteristics of street facades. Low-rise commercial areas commonly found in the Central Area, such as Chinatown and Haji Lane, and high-rise commercial areas like Raffles Place and City Hall, can be further distinguished based on the size and proximity of light spots in road scenes. Due to differences in street height-to-width ratios and the principle of objects appearing larger when closer, in narrow low-rise commercial areas, light sources closer to the camera on street facades appear as larger lighted spots above the horizon line. Conversely, in high-rise commercial areas, where streets are wider, light sources on street facades are reflected in the images as dimmer and closer to the horizon line (see **??**).

In industrial parks, highways, and campus environments, most road scenes are characterized by lower total luminosity, smaller lighted spot area, and light spots closer to the horizon line (Cluster 1). These scenes typically have fewer or no buildings enclosing them and can be in lack of prominent lighting sources. As for the differences among them, highways have a higher proportion of road scenes

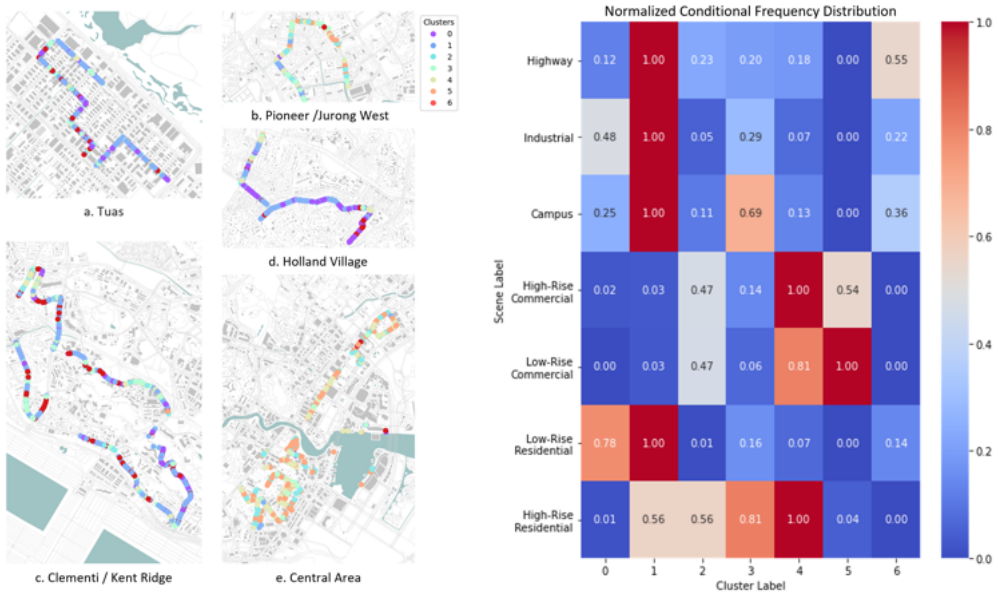

Figure 8: Spatial distribution of different lighting pattern clusters (left) and their conditional frequency distribution in different functional scenarios (right). Specifically: (a) Tuas is a typical industrial area; (b) Pioneer and Jurong West are modern residential areas characterized by high-rise blocks; (c) Holland Village is characterized by low-rise residential buildings; (d) Clementi and Kent Ridge encompass diverse road scenarios, including university campus, highway, and high-rise residential community; and (e) the Central Area is characterized by a mix of low-rise and high-rise commercial buildings. We summarize and normalize the conditional frequencies of different clusters appearing in the functional scenarios above to illustrate the association between lighting patterns and activity scenarios, as shown in the right plot. Source of the basemap:OpenStreetMap.

with higher brightness and light spots (Cluster 6), where streetlights overhead often serve as the main lighting source. The industrial park and the campus are very similar in lighting patterns, while campus scenes are brighter, as indicated by the higher frequency of Cluster 3.

Furthermore, different types of residential neighborhoods in Singapore may exhibit contrasting lighting characteristics. For low-rise residential areas, most road scenes have lower brightness, smaller light spots, and light spots close to the horizon line (Cluster 1). However, a certain proportion of scenes are in low-light environments with relatively higher light spots (Cluster 0). Singapore's current low-rise residential areas generally follow the colonial-era planning traditions, with narrow roads and closely packed independent or terraced houses with walls along both sides of the street. These areas have strong enclosure from the street interface but weaker service functions, which may explain that why most of the scenes are not fully illuminated. In contrast, high-rise residential areas show a more diverse lighting pattern, with significantly brighter lighting patterns (Cluster 2, 3, 4) and the low-brightness lighting patterns that dominate in low-rise areas (Cluster 1) both having a prominent presence. Singapore's high-rise residential areas emphasize vertical density, the mix of commercial and residential functions, and the modernity of transportation and lighting facilities. Thus, the complex lighting characteristics in high-rise residential area may be influenced by three main types of light sources: the illumination from service interfaces of community commercial and public facilities; resident window lights and the constant illumination maintained in corridors for safety reasons; and the lamp lighting serving the extensive commuter traffic. It is also noticeable that, high-rise residential areas and commercial areas show similar proportion of cluster 2, which suggests scenarios with considerably high brightness. Though different in distribution of other lighting patterns, there are comparable lighting intensity in high-rise residential areas and commercial areas in Singapore.

4.2. Brightness Prediction

4.2.1. Model Performance

We assess the performance of various models in predicting nighttime brightness based on daytime SVIs. Table 1 presents a comparison of MAE, RMSE and MSE for models on both training and testing datasets. The EfficientNetB3 model achieved the lowest RMSE and MSE scores and a significantly lower MAE score on the testing set, leading it to be selected as the model for further nighttime brightness prediction. Machine learning models performed worse compared to deep learning models. While vectorized contextual information, such as road

classes and segmented street view elements, also contributes to inferring nighttime brightness, utilizing daytime SVI as input proves to be a more direct and efficient approach.

It is observed that most models present a tendency of over-fitting on the test dataset. To gain further insight into the potential causes and impacts of overfitting, we conducted an error distribution analysis on the EfficientNetB3 model. Figure 9 displays the spread of prediction errors across the training, validation, and testing datasets. On the testing and validation sets, the errors follow a broader distribution ranging from -5 to 5, indicating that the model has a tendency to predict higher brightness values for dark scenes and lower values for bright scenes. Figure 10 provides a closer examination of specific instances of overestimation and underestimation, showcasing their corresponding daytime SVIs and spatial distribution. An interesting pattern emerges in open, low-density areas with street lamps at regular intervals. These street lamps, while occupying only a small portion of the SVI pixels, play a significant role in determining the brightness of corresponding images. Their impact is pronounced when they are situated near the photo collection points or directly above it. Nevertheless, for the majority of other scenarios not dotted with street lamps, the model performs better. The bias introduced by street lamps is relatively contained due to their fixed placement at regular intervals. These lamps influence only specific, localized areas within the SVIs, leaving the majority of the image unaffected.

Models	MAE		RMSE		MSE	
	Train	Test	Train	Test	Train	Test
OLS	1.3321	1.3407	1.6598	1.6605	2.7549	2.7572
Random Forest	0.5009	1.3605	0.6245	1.6812	0.3900	2.8263
XGBoost	0.2618	1.4802	0.3649	1.8505	0.1331	3.4242
EfficientNetB0	0.4022	1.3190	0.4998	1.6362	0.2498	2.6770
EfficientNetB3	0.2616	1.2815	0.3313	1.5687	0.1098	2.4607
Vision Transformer l32	0.5794	1.4172	0.7316	1.7624	0.5352	3.1060
Vision Transformer b16	0.3781	1.2696	0.4733	1.5724	0.2240	2.4726
VGG16	1.3083	1.3718	1.6293	1.6896	2.6545	2.8549
ResNet50V2	0.2055	1.3114	0.2648	1.6240	0.0701	2.6373

Table 1: Model performance comparison.

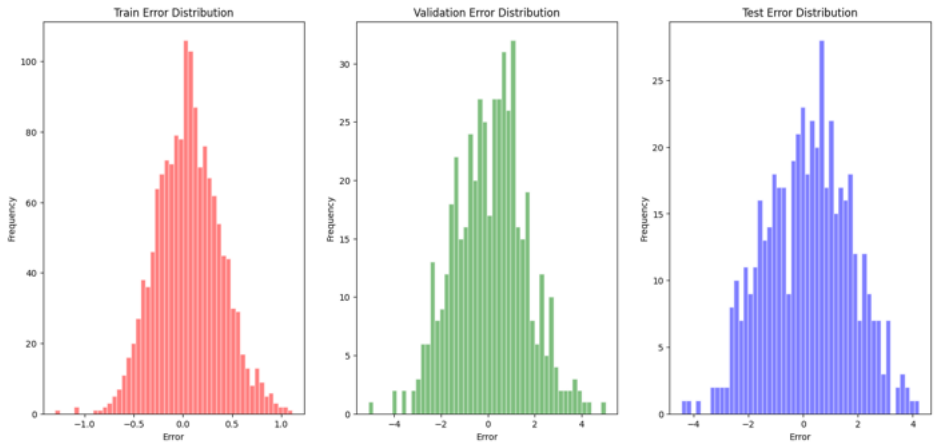

Figure 9: Error distribution across training, validation and test sets.

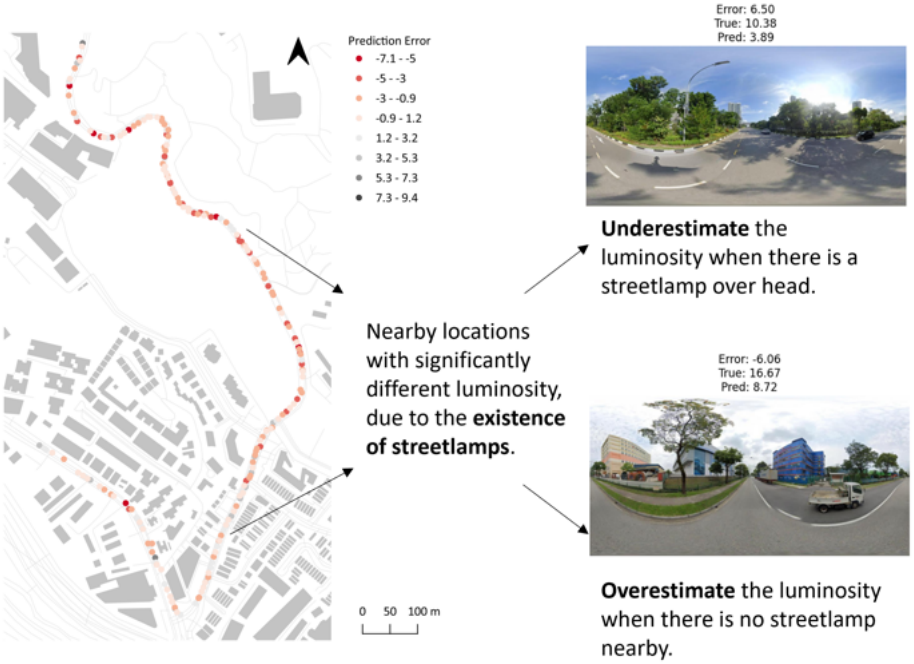

Figure 10: Samples of overestimated and underestimated brightness values. Source of the basemap: OpenStreetMap.

4.2.2. Model Scaling

To gain insights into the nighttime lighting landscape at the street level on a larger scale, we further scaled the best model to cover daytime SVIs throughout Singapore. By comparing the spatial and data distribution of predicted nighttime brightness with nighttime brightness obtained from SDGSAT-1 satellite imagery, we aim to understand whether the predicted brightness can be a valid representation of night time lighting landscape, and to what extent the two brightness features convey the same information.

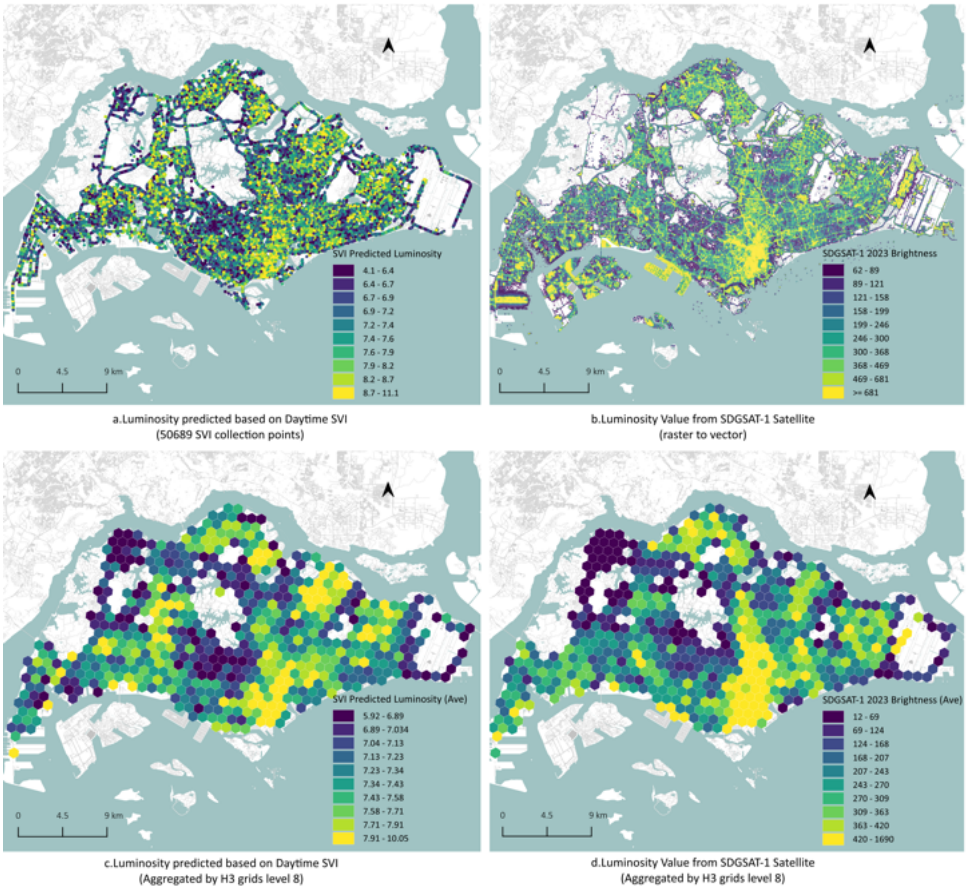

Figure 11: A comparison of predicted brightness and the satellite derived brightness. Source of the basemap: OpenStreetMap.

Figure 11 illustrates the spatial distribution of the predicted street-level brightness and the satellite based NTL brightness, and their aggregated mean values

by H3 hexagon grids. The resolution of H3 grids is set to level 8, with an average hexagon area of 0.737 km^2. All of the features are divided into 10 quantiles and visualized on a consistent scale for comparative analysis. It is found that the predicted brightness generally follow similar spatial distribution pattern with the satellite based NTL brightness. However, there are also significant discrepancies in local areas.

4.3. Further Analysis on the Predicted Brightness

The study investigates the distinct features of SVI predicted brightness, by interpreting its discrepancy with satellite derived brightness and exploring its relation with multiple urban activities. For the first task, an OLS regression model is fitted based on the aggregated values, to model the potential linear association between the SVI predicted brightness and the satellite based brightness.Then residual distribution of the model presents a refined look of the discrepancies between two brightness measurements. Spatial auto-correlation analysis is applied to the residuals to check the potential spatial pattern in the discrepancies.

According to the analysis, the R-squared of the OLS model is 0.3644, with the coefficient of mean brightness being 0.6228 and the corresponding probability below 0.05. The result suggests that every unit change in predicted brightness might explain a 0.62 change in the same direction of satellite derived brightness, and the two show a significant and moderate correlation. Figure 12a illustrates the spatial distribution of the residuals in the Singapore scale and n Figure12b, the Local Moran's I analysis highlights significant high-high and low-low clustering of residuals in the overestimated and underestimated areas. It is found that the predicted brightness and satellite derived brightness are aligned well with each other in most of the cells. There are significant and continuous discrepancies mainly exist on the Singapore Central Area and port terminal area on the south, and the Changi Airport area on the east, showcasing an underestimates of SVI predicted brightness to the satellite derived brightness. Besides, several continuous grids showing overestimates are located on the west and north of Singapore. According to the analysis above, it is argued that the predicted brightness can be meaningful proxy of urban lighting, while its discrepancy with satellite derived brightness in local urban areas require further explanation, and in fact, as we will discuss in the next continuation, is the affirmation of the uniqueness and usefulness of the novel perspective we introduce.

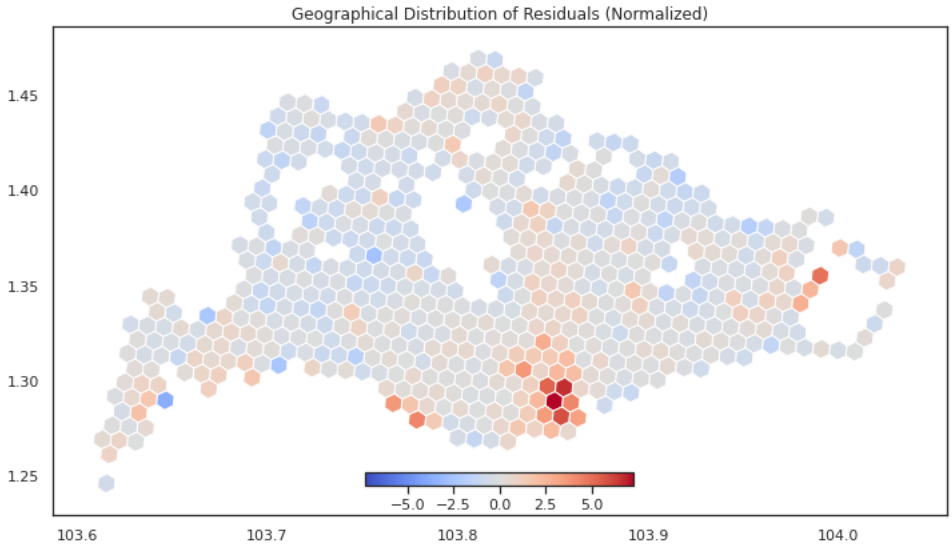

(a) Spatial distribution of residuals in Singapore.

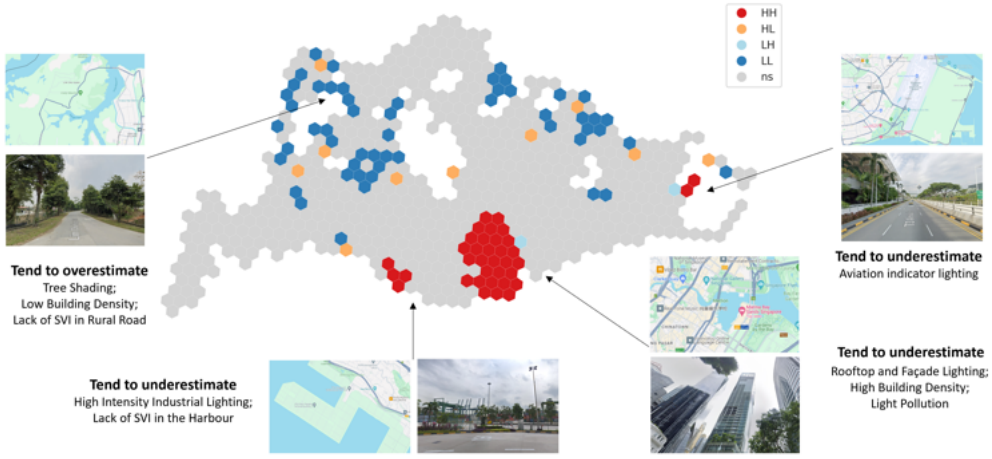

(b) Significant spatial clustering detected among the residual distribution.

Figure 12: Residual analysis for OLS regression model, suggesting the discrepancies between the traditionally used nighttime satellite imagery and the street-level counterpart that we study in this paper. Source of the imagery and basemaps in the examples: Google Street View and Google Maps.

4.3.1. Discrepancy between Brightness Distributions

We explain the discrepancies between street view imagery and satellite imagery in reflecting nighttime brightness characteristics based on the differences in their imaging features. These imaging differences can be specifically described as, different imaging perspectives and targeted light sources, different spatial coverage, and different imaging resolution and continuity. We provide a detailed discussion on how these differences in imaging characteristics contribute to the observed discrepancies in two brightness distribution.

Initially, it is posited that the observed discrepancies between street view and satellite imagery in capturing nighttime lighting information stem from their differing observational perspectives. Street view imagery records light at ground level, encompassing a spherical perspective where street lamps, building facades, and vehicle headlights are primary light sources. In contrast, satellite imagery captures a broader, top-down view of urban areas, emphasizing light sources elevated above ground level and unobscured by trees or buildings. Correlating residual distribution with real-world map reveals that the urban functions and morphology are highly homogeneous and unique in the highlighted area may have derived from special lighting pattern sensed differently by street view imagery and satellite imagery. For instance, in the Central Area with high development intensity and densely distributed with high-rise commercial building, there are significantly more rooftop and facade lighting on the higher elevation, which may overshadow the street-level lighting in the satellite imagery, leading to underestimation. In contrast, the rural road areas in northern Singapore, characterized by dense vegetation, may obscure street-level lights from satellite detection, leading to overestimation in these areas. In the port and airport areas, intense industrial and aviation lighting, often inaccessible to street-level imagery, results in an underrepresentation of SVI predicted brightness to the satellite derived brightness.

In addition, the study also considers the role of coverage difference between SVI and satellite imagery in explaining the distribution discrepancies of the two brightness features. The NTL satellite imagery can often cover the whole urban boundary and reflect lighting information from both roads and blocks' inner environment within a grid. While the daytime SVIs are generally available on public roads, with its city-scale coverage dependent on the density and distribution of road network and with a evident focus on the road environment. It is assumed that significant coverage difference between the two imagery types, especially the missing of SVI coverage, can result in extra discrepancies in the brightness distribution.

By creating and merging 30 m buffers for daytime SVI collection points, and calculating the proportion of buffer area to each grid, the study first measures the daytime SVI coverage in Singapore. Then the residuals from the initial OLS model are divided in 4 groups according to 4 quantiles of SVI coverage perception and are compared in box plot. As shown in Figure 13a, the daytime SVIs show an unbalanced distribution from south to north and from west to east. The rural and industrial area on the west of Singapore have significantly lower SVI coverage compared to the middle and east of Singapore. The areas are featured with farms, natural reserves and new-developed port and industrial areas, where latest SVI collection can be insufficient. According to the box plots in Figure 13b, when the SVI coverage is low, the satellite derived brightness are tended to be overestimated, with residuals showing a lower mean value and in lower general distribution in the axial. When there is a high SVI coverage, most of the NTL brightness can be correctly estimated, though there can be more high-residual outliers.

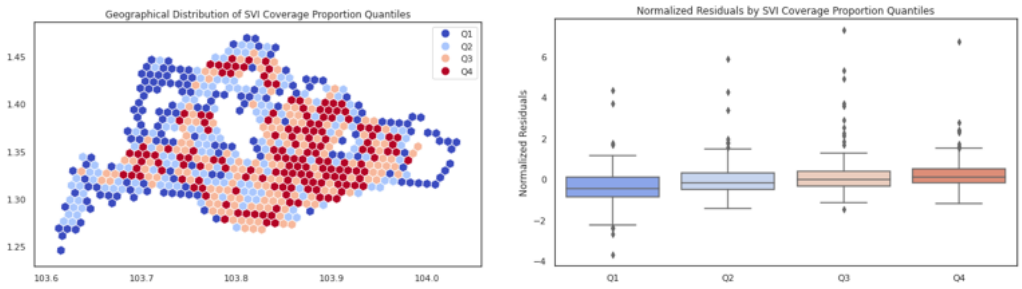

(a) The unbalanced SVI coverage in Singapore.

(b) Residual distribution under SVI coverage.

Figure 13: Relation between OLS model residuals and SVI coverage.

Beyond the discrepancies caused by imaging perspective and coverage difference in certain urban areas, the imaging difference in resolution and continuity in street view imagery and satellite imagery can also play a positive role. The spatial auto-correlation analysis in Figure 12c has revealed the existence of spatial neighboring effect unexplained in the residuals from the OLS model. It is assumed that the geographic neighboring effect of urban lighting pattern is overwhelmingly embodied in the satellite imagery, while not fully represented in the solely captured SVIs. Specifically, satellite imagery captures the lighting characteristics from a continuous geographical space at one time. The satellite derived brightness in a hexagon grid may not only be the representation of the lights from the grid itself, but also affected by light sources from nearby grids. Typically, the problems can

be reflected as the light pollution or glare occurring in low-resolution satellite imagery. In contrast, the nighttime SVIs capture lighting pattern at discontinuous local spaces and at multiple times. There can be relatively weaker representation of spatial continuity in the SVI predicted brightness, however the spatial resolution can be higher.

To comprehensively test the hypothesis above, a spatial lag regression model is applied to refine the correlation between SVI predicted brightness and satellite-derived brightness, considering geographic neighboring effects, SVI coverage differences, and varying urban development intensities and functions. For each hexagon grid, the average of predicted brightness from the Queen neighboring grids was calculated as a spatial lag variable. Additional independent variables include the SVI buffer area proportion, the maximum Gross Plot Ratio (GPR) per grid, and the presence of ports and airports in the grid. The study also incorporates VIIRS-DNB and Luojia-1 NTL images with different resolutions to assess imagery resolution impacts on brightness feature extraction and model fitting. The comparative analysis of Adjusted R2 metrics in Table 2 reveals that spatial lag models consistently yield higher R2 scores than OLS models, highlighting the importance of spatial neighboring characteristics in the relationship between SVI predicted and satellite-derived brightness. Models using lower-resolution imagery show more significant improvements in Adjusted R2 scores in spatial-lag models than OLS models, suggesting that low-resolution nighttime images may more substantially obscure actual lighting conditions due to radiance and noise issues. Additionally, by accounting for the uneven distribution of SVIs, GPR, and port/airport facilities, both OLS and spatial-lag models demonstrate improved fits, supporting the three hypothesis proposed to explain the discrepancies.

4.3.2. Relation between Brightness and Activities

The aforementioned analysis attempts to reveal the differences in how street view images and satellite imagery capture urban lighting characteristics. The further questions are, what is the practical significance of these differences and how can brightness predicted from SVI help us better understand the nocturnal functions and activities of a city? Figure 14 demonstrates the correlation between SVI predicted brightness, satellite-derived brightness, and the number of various types of Points of Interest (POIs) within each grid. At urban scale, the POI counts in shopping and food, culture and tourism, and public services and amenities show significantly higher correlation with satellite-derived brightness than the SVI predicted brightness. For POI health and education POI, the correlation of SVI predicted brightness is broadly on par with satellite-derived brightness. While for

	SDGSAT–1 40m	Luojia-1 130m	VIIRS–DNB 500m
OLS Regression			
Adjusted R2			
SVI Brightness	0.3195	0.3829	0.2944
SVI Brightness | SVI Coverage	0.3805	0.5162	0.3636
SVI Brightness | SVI Coverage | GPR	0.5106	0.6227	0.4018
SVI Brightness | SVI Coverage | GPR | Port/Airport	0.5421	0.6546	0.4680
Spatial Lag Regression			
Adjusted R2			
SVI Brightness	0.3920	0.4879	0.4168
SVI Brightness | SVI Coverage	0.4262	0.5726	0.4548
SVI Brightness | SVI Coverage | GPR	0.5180	0.6383	0.4622
SVI Brightness | SVI Coverage | GPR | Port/Airport	0.5515	0.6742	0.5359

Table 2: A summary of adjusted R2 across different OLS and spatial-lag regression models.

recreation and sports POI, the SVI predicted brightness shows a notably stronger correlation than the satellite derived brightness. The detailed classification method of POI is introduced in the Appendix B.

These findings first suggest that the two types of brightness differ in their ability to map various urban activities. This disparity may partly stem from the imaging differences discussed earlier. On the other hand, it is also related to the distribution and clustering patterns of various urban activities. In Singapore, for instance, influenced by the city's planning traditions, shopping, dining, and various daily convenience services are typically concentrated in shopping malls and neighborhood hubs, and exhibiting a high degree of geographical concentration in specific urban and regional centers (Sim et al., 2002; Hee and Ooi, 2003). Since these services are often indoors and not street-facing, there can be weaker correlation of SVI predicted brightness with such services. While in the satellite imagery, the spatial concentration of the activities, through their lighting features, can be better captured at a global scale, which interpret a generally higher correlation score. Conversely, facilities like hospitals, schools, and parks, which have independent layout requirements and include outdoor areas, may have their nighttime lighting characteristics better captured by SVIs. The facilities and related activities are not evident in NTL imagery, reported as in previous research.

Furthermore, it is found that as the resolution of satellite imagery decreases, its brightness' correlation with various POI counts generally diminishes. This indicates that the resolution of satellite imagery may have an important impact on its

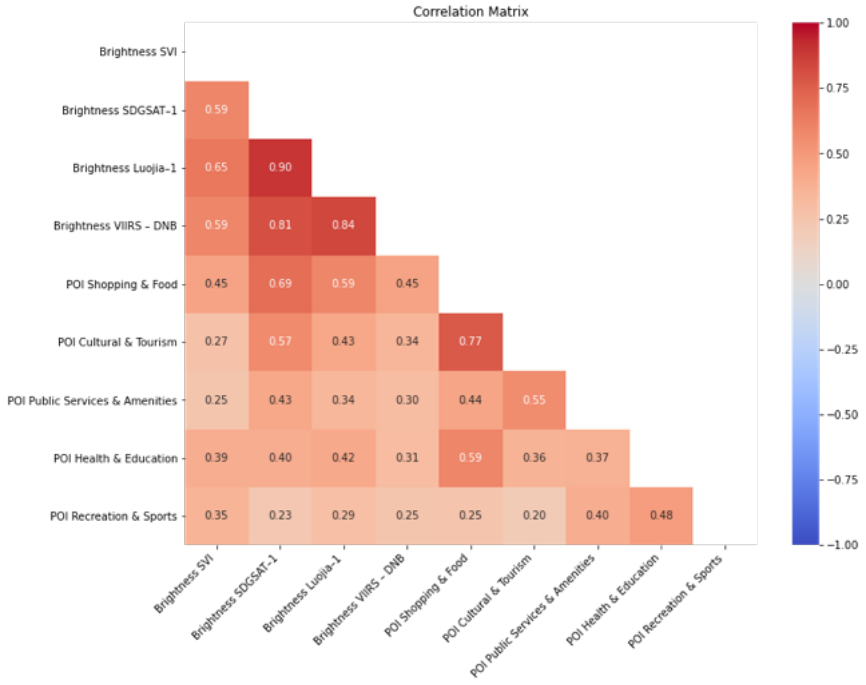

Figure 14: Correlation between different brightness features and different POI counts.

ability to map urban activities. Compared to the low resolution NTL imagery suffering more from the light pollution, high resolution NTL imagery are expected to more precisely capture the intensity and location of lighting sources, which contributes to a better mapping of urban activities. However, the high-resolution NTL imagery can be rare and often limited as open-sourced data in current urban research. In light of this, by comparing the correlation scores of SVI predicted brightness and different satellite derived brightness, with POI count, it is possible to roughly estimate SVI predicted brightness 's potential and compatibility, in replacing satellite imagery in revealing characteristics of nocturnal urban activities. While the correlation of POI counts with SVI predicted brightness is overall weaker than that with high-resolution satellite imagery's brightness, from SDGAST-1 and Luojia-1, it is on par with and in certain activity categories exceeds, the brightness from the widely used but lower precision VIIRS-DNB imagery. In summary, SVI predicted brightness can serve as a novel nighttime urban lighting intensity indicator, and hold significant and competitive potential in revealing characteristics of nocturnal urban activities compared to the NTL imagery.

5. Discussion

5.1. Diverse and Consistent Urban Lighting patterns Reflected in Nighttime SVIs

The research endeavors to apply clustering methods, to explore potential homogeneous patterns within street-level lighting landscapes. The measured luminosity of the scene and the area of lighted spots extracted from nighttime SVIs, are identified as primary attributes for differentiating lighting patterns, whereas the average distance of spots from the image centroids aids in subdividing different patterns. Based on the analysis in the Section 4.1.2, there are seven generic lighting patterns extracted from the nighttime SVIs. We can discern that each urban functional space can be typically described by one or two primary lighting patterns, characterizing their usual illumination features, and distinguished by another possible secondary lighting pattern from other functional scenes. For different urban functional scenes, the dominant lighting pattern may share commonalities, depending on the human activities and location's characteristics within the scene. For example, Cluster 1 is predominantly lit by industrial parks, highways, and university campuses; Cluster 5 is prevalent in low-rise commercial areas, high-rise commercial areas, and high-rise residential areas. The aforementioned findings structurally describe the mapping between street-level urban functional characteristics and generic lighting patterns, making a pioneering contribution to the study of the nighttime urban built environment and human activities. The study reveals the readability of urban lighting landscape, and also highlights the potential value of collecting nighttime SVIs in a larger-scale and identifying different lighting patterns as prototypes.

5.2. SVI based Brightness vs Satellite based Brightness

This study trains deep learning models for predicting Singapore's nighttime brightness features at city scale based on daytime SVIs. It further probes the relationship between SVI-predicted brightness and satellite derived brightness, aiming to unravel the significance of nighttime SVIs as a potential complementary of nighttime satellite images. Regression analysis yields Adjusted R^2 values of 0.3195 and 0.3920 for the OLS and spatial lag models respectively, indicating a significant, moderate correlation. While global spatial consistency is observed, significant local discrepancies highlight the distinct but related dimensions captured by SVIs and satellite imagery. These differences are attributed to variations in imaging perspectives, spatial coverage, and resolution and continuity between the two sources. In addition, by linking the POI count with the brightness distribution, the study reveals that the two types of brightness differ in their ability

to map various urban activities. SVI predicted brightness shows stronger correlation with POIs that have requirements in independent layouts and outdoor fields, such as schools, hospitals, and parks. Besides, the lower the resolution of satellite imagery, the more similar the performance between SVI predicted brightness and satellite derived brightness in mapping the urban activities. The above findings suggest that the SVI predicted brightness can be competitive nighttime lighting indicators to reveal the urban activity features. Especially, it is argued that when there is a lack of high-resolution NTL image, or the street-based distribution are stressed for urban activities, the SVI predicted brightness can be a better fit compared to the traditional satellite derived brightness indicators.

5.3. Potential Applications and Limitations of Nighttime SVI

Based on our investigation, there are promising applications of nighttime SVI, and thus we believe that this latent urban dataset warrants more attention. By identifying typical lighting patterns and sources via Nighttime SVI, we can optimize light placement and intensity to enhance regional characteristics (Alves, 2007), or reduce light trespass in densely populated residential areas, addressing the potential health concerns (Vallée et al., 2020; Chen et al., 2020; Sung, 2022). With its unique horizontal perspective, Nighttime SVI serves as a valuable data source for assessing window lighting and estimating vacancy rates in residential and commercial properties. This is significant for urban planners or policymakers as it provides insights into urban ghost cities (Yin et al., 2024; Shi et al., 2020) or hollowing phenomena (Batty, 2023). However, personal privacy may be compromised due to this granular observation. Nighttime SVI can also be applied as direct material for auditing local environment in crime prevention and environmental psychology research. Additionally, nighttime SVI can effectively cover areas with dense tree canopies or tall buildings, where NTL data may fail to achieve a sufficient coverage. Combining SVI with satellite imagery offers a comprehensive view of urban lighting across different altitudes and dimensions, potentially improving traditional NTL data applications like energy consumption modeling (Wang and Lu, 2021) and economic observation (Xu et al., 2021).

Despite these potentials, we must also acknowledge the complexities of urban nighttime environments and the possible limitations of Nighttime SVI. Urban lighting levels can fluctuate between early evening and late night due to changes in shop activity, streetlight intensity, and traffic flow, making the collection timestamp crucial for accurate analysis. Geographic factors, including climate and seasonal variations, further influence lighting conditions. For example, dense summer foliage in temperate regions may obstruct streetlights and building illumi-

nation, whereas such obstructions are minimal in winter. The complexity and temporal dynamics of urban lighting environments present challenges for relying solely on static nighttime images for urban sensing. Nevertheless, similar issues are also present in traditional practices based on NTL data.

6. Conclusion

This paper puts forward the idea of using street-level imagery taken during nighttime as a potentially useful dataset for sensing urban lighting conditions, which has been ignored so far, despite the immense popularity of its daytime counterpart. Collecting and utilizing nighttime SVIs as primary data source, this study analyzes the street-level urban lighting landscape at city-scale from human perspective, and explores its extensive connections with urban functional scenario, built environment forms, and activity distribution. Besides pioneering this paradigm, the main contributions of this research are addressing the limitations in nocturnal urban studies that have long relied on NTL satellite imagery, suffering from a singular observation perspective and low data resolution, and systematically and insightfully investigating the basic properties of nighttime SVIs and their relationship with other conventional urban data sources. It is argued that nighttime SVI can be the basis of a novel urban sensing paradigm and provide feasible information in expanding our cognitive dimensions of urban environment and activities.

Our investigation highlights the potential applications of nighttime SVI for a more comprehensive understanding of urban lighting. Firstly, nighttime SVI can serve as an independent medium for describing and measuring the street-level lighting landscape, capturing the distribution of light sources along the urban vertical dimension. This will significantly enhance studies that require high-detail investigations of lighting environments, particularly in areas such as the health impacts of light pollution and crime prevention. Secondly, by integrating nighttime SVI with daytime SVI and leveraging deep learning technologies, it can complement NTL satellite imagery by inferring street-level lighting intensity across large spatial scales. This application offers differentiated urban activity information and perspectives that may be overlooked by NTL, while potentially better supporting traditional NTL applications, such as sensing urban vitality and functional structure, and predicting energy consumption.

Nonetheless, being the first such study, it has some limitations that offer opportunities for future work. It does not consider the role of nighttime light color characteristics in differentiating urban functional areas. This issue stems mainly

from the complexity and instability of nighttime color measurement. However, specific light color spectra and color richness could indicate different urban activities, making this a viable direction for future research. Additionally, the fact that all nighttime SVIs were collected from Singapore could impact the generalizability of brightness prediction models to other global cities. Future research could benefit from collecting nighttime SVI from a broader range of sources. Beyond manual collection, potential supplemental sources include nighttime SVIs from Mapillary and nighttime city walk videos from open access platforms. Diverse datasets will help improve the robustness of the models.

Acknowledgments

We thank our colleagues at the NUS Urban Analytics Lab for the discussions. Rudi Stouffs, Winston Yap and Maxim Khomiakov are gratefully acknowledged for the discussions on the initial concept of the research and the development of deep learning approaches. The first author is supported by the National University of Singapore under the President Graduate Fellowship. This research is part of the project Large-scale 3D Geospatial Data for Urban Analytics, which is supported by the National University of Singapore under the Start Up Grant R-295-000-171-133. It is acknowledged that the SDGSAT-1 data are kindly provided by International Research Center of Big Data for Sustainable Development Goals (CBAS).

Author contributions

Zicheng Fan: Conceptualization; Methodology; Software; Validation; Formal analysis; Investigation; Data Curation; Writing - Original Draft; Visualization. **Filip Biljecki:** Conceptualization; Methodology; Investigation; Writing - Review & Editing; Visualization; Supervision; Project administration; Funding acquisition.

Appendix A. Silhouette Analysis

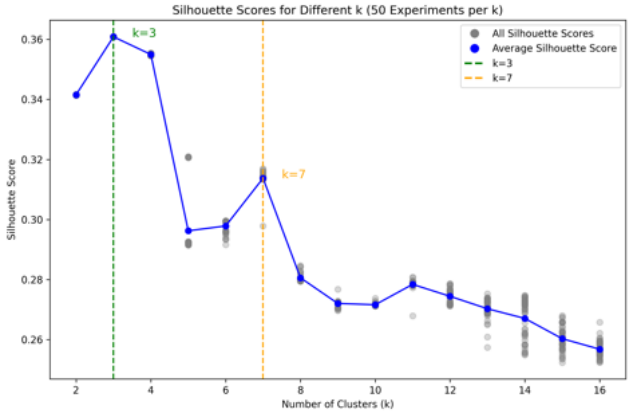

Figure A.15: Average silhouette scores for different k (50 Experiments per k). Though k=3 has the highest silhouette score, we choose k=7 for better diversity.

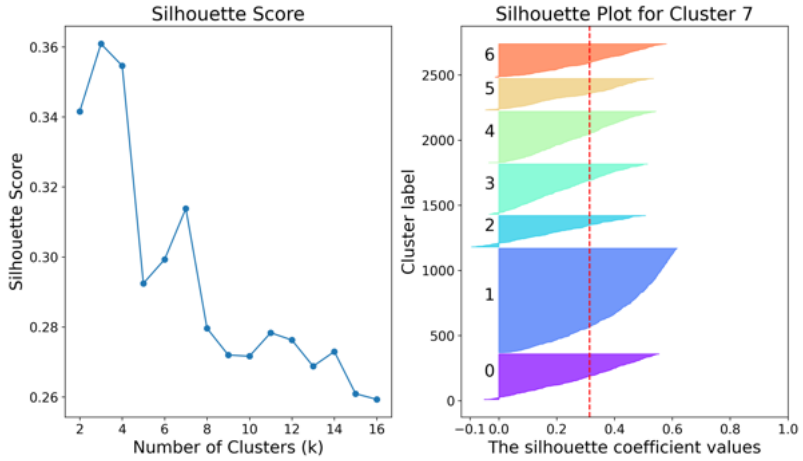

Figure A.16: Results from the silhouette analysis with k=7 and random seed = 238.

Feature	F-statistic	p-value
Total Area	691.9921	0.0
Total Luminosity	869.8054	0.0
Average Distance	686.0040	0.0

Table A.3: ANOVA results for different lighting features across clusters.

Group 1	Group 2	Mean Diff.	p-adj	Reject
0	1	-4194.3325	0.0	True
0	2	24838.0110	0.0	True
0	3	4588.1625	0.0	True
0	4	22391.5417	0.0	True
0	5	40916.2308	0.0	True
0	6	3258.4487	0.0127	True
1	2	29032.3435	0.0	True
1	3	8782.4950	0.0	True
1	4	26585.8742	0.0	True
1	5	45110.5633	0.0	True
1	6	7452.7812	0.0	True
2	3	-20249.8485	0.0	True
2	4	-2446.4693	0.1514	False
2	5	16078.2198	0.0	True
2	6	-21579.5623	0.0	True
3	4	17803.3792	0.0	True
3	5	36328.0683	0.0	True
3	6	-1329.7138	0.838	False
4	5	18524.6891	0.0	True
4	6	-19133.0930	0.0	True
5	6	-37657.7822	0.0	True

Table A.4: Tukey's HSD Test results for total area across clusters.

Group 1	Group 2	Mean Diff.	p-adj	Reject
0	1	-2.8601	0.0001	True
0	2	33.3785	0.0	True
0	3	13.3819	0.0	True
0	4	3.3151	0.0001	True
0	5	13.4703	0.0	True
0	6	21.7076	0.0	True
1	2	36.2387	0.0	True
1	3	16.2420	0.0	True
1	4	6.1752	0.0	True
1	5	16.3305	0.0	True
1	6	24.5677	0.0	True
2	3	-19.9967	0.0	True
2	4	-30.0634	0.0	True
2	5	-19.9082	0.0	True
2	6	-11.6710	0.0	True
3	4	-10.0668	0.0	True
3	5	0.0885	1.0	False
3	6	8.3257	0.0	True
4	5	10.1552	0.0	True
4	6	18.3925	0.0	True
5	6	8.2372	0.0	True

Table A.5: Tukey's HSD Test results for total luminosity across clusters.

Group 1	Group 2	Mean Diff.	p-adj	Reject
0	1	-25.5540	0.0	True
0	2	-11.6235	0.0	True
0	3	-17.3549	0.0	True
0	4	-18.3024	0.0	True
0	5	-7.6999	0.0	True
0	6	3.4640	0.0	True
1	2	13.9306	0.0	True
1	3	8.1992	0.0	True
1	4	7.2517	0.0	True
1	5	17.8542	0.0	True
1	6	29.0180	0.0	True
2	3	-5.7314	0.0	True
2	4	-6.6789	0.0	True
2	5	3.9236	0.0	True
2	6	15.0874	0.0	True
3	4	-0.9475	0.7395	False
3	5	9.6550	0.0	True
3	6	20.8188	0.0	True
4	5	10.6025	0.0	True
4	6	21.7663	0.0	True
5	6	11.1638	0.0	True

Table A.6: Tukey's HSD Test results for average distance across clusters.

Appendix B. A Re-classification of POI Types

New POI Types	Original POI Types
Shopping & Food	cafe, food_court, restaurant, fast_food, bakery, bar, pub, convenience, furniture_shop, supermarket, outdoor_shop, doityourself, florist, bicycle_shop, bookshop, chemist, clothes, computer_shop, department_store, greengrocer, jeweller, pharmacy, shoe_shop, gift_shop, kiosk, beauty_shop, car_dealership, garden_centre, butcher, stationery, mobile_phone_shop, toy_shop, general, mall, newsagent, arts_centre
Cultural & Tourism	artwork, museum, cinema, theatre, nightclub, theme_park, zoo, stadium, hotel, guesthouse, hostel, motel, tourist_info, viewpoint, monument, observation_tower, lighthouse, ruins, battlefield, picnic_site, camp_site, chalet
Public Services & Amenities	atm, bank, travel_agent, police, fire_station, town_hall, public_building, library, embassy, prison, community_centre, post_office, post_box, toilet, drinking_water, waste_basket, recycling, recycling_paper, recycling_glass, bench, vending_machine, vending_any, telephone, car_rental, car_sharing, car_wash, bicycle_rental
Health & Education	doctors, clinic, hairdresser, dentist, veterinary, school, kindergarten, college, university
Recreation & Sports	playground, swimming_pool, sports_centre, ice_rink, dog_park, pitch, park

Table B.7: New classification scheme of POI types. The original POI types are re-classified to five new types, based on their similarity and difference in activity features.

References

Alves, T., 2007. Art, Light and Landscape New Agendas for Urban Development. European Planning Studies 15, 1247–1260. URL: https://doi.org/10.1080/09654310701529243, doi:10.1080/09654310701529243. publisher: Routledge _eprint: https://doi.org/10.1080/09654310701529243.

Anoosheh, A., Sattler, T., Timofte, R., Pollefeys, M., Gool, L.V., 2019. Night-to-Day Image Translation for Retrieval-based Localization, in: 2019 International Conference on Robotics and Automation (ICRA), IEEE, Montreal, QC, Canada. pp. 5958–5964. URL: https://ieeexplore.ieee.org/document/8794387/, doi:10.1109/ICRA.2019.8794387.

Ao, Y., 2019. Fully convulutional networks for street furniture identification in panorama images. URL: http://essay.utwente.nl/85874/. publisher: University of Twente.

Aravena Pelizari, P., Geiß, C., Aguirre, P., Santa María, H., Merino Peña, Y., Taubenböck, H., 2021. Automated building characterization for seismic risk assessment using street-level imagery and deep learning. ISPRS Journal of Photogrammetry and Remote Sensing 180, 370–386. URL: https://www.sciencedirect.com/science/article/pii/S0924271621001817, doi:10.1016/j.isprsjprs.2021.07.004.

Batty, M., 2023. The post-pandemic world: Are big cities hollowing out? Environment and Planning B: Urban Analytics and City Science 50, 1409–1412. URL: https://doi.org/10.1177/23998083231188188, doi:10.1177/23998083231188188. publisher: SAGE Publications Ltd STM.

Bennett, M.M., Smith, L.C., 2017. Advances in using multitemporal night-time lights satellite imagery to detect, estimate, and monitor socioeconomic dynamics. Remote Sensing of Environment 192, 176–197. URL: https://www.sciencedirect.com/science/article/pii/S0034425717300068, doi:10.1016/j.rse.2017.01.005.

Biljecki, F., Ito, K., 2021. Street view imagery in urban analytics and GIS: A review. Landscape and Urban Planning 215, 104217. URL: https://www.sciencedirect.com/science/article/pii/S0169204621001808, doi:10.1016/j.landurbplan.2021.104217.

Biljecki, F., Zhao, T., Liang, X., Hou, Y., 2023. Sensitivity of measuring the urban form and greenery using street-level imagery: A comparative study of approaches and visual perspectives. International Journal of Applied Earth Observation and Geoinformation 122, 103385. URL: https://www.sciencedirect.com/science/article/pii/S1569843223002091, doi:10.1016/j.jag.2023.103385.

Breiman, L., 2001. Random Forests. Machine Learning 45, 5–32. URL: https://doi.org/10.1023/A:1010933404324, doi:10.1023/A:1010933404324.

Brostow, G.J., Fauqueur, J., Cipolla, R., 2009. Semantic object classes in video: A high-definition ground truth database. Pattern Recognition Letters 30, 88–97. URL: https://www.sciencedirect.com/science/article/pii/S0167865508001220, doi:10.1016/j.patrec.2008.04.005.

Chalfin, A., Hansen, B., Lerner, J., Parker, L., 2022. Reducing Crime Through Environmental Design: Evidence from a Randomized Experiment of Street Lighting in New York City. Journal of Quantitative Criminology 38, 127–157. URL: https://doi.org/10.1007/s10940-020-09490-6, doi:10.1007/s10940-020-09490-6.

Chen, S., Wei, M., Dai, Q., Huang, Y., 2020. Estimation of Possible Suppression of Melatonin Production Caused by Exterior Lighting in Commercial Business Districts in Metropolises. LEUKOS 16, 137–144. URL: https://doi.org/10.1080/15502724.2018.1523013, doi:10.1080/15502724.2018.1523013. publisher: Taylor & Francis _eprint: https://doi.org/10.1080/15502724.2018.1523013.

Chen, T., Guestrin, C., 2016. XGBoost: A Scalable Tree Boosting System, in: Proceedings of the 22nd ACM SIGKDD International Conference on Knowledge Discovery and Data Mining, pp. 785–794. URL: http://arxiv.org/abs/1603.02754, doi:10.1145/2939672.2939785. arXiv:1603.02754 [cs].

Cheng, L., Yuan, Y., Xia, N., Chen, S., Chen, Y., Yang, K., Ma, L., Li, M., 2018. Crowd-sourced pictures geo-localization method based on street view images and 3D reconstruction. ISPRS Journal of Photogrammetry and Remote Sensing 141, 72–85. URL: https://www.sciencedirect.com/science/article/pii/S0924271618301102, doi:10.1016/j.isprsjprs.2018.04.006.

Cho, Y., Ryu, S.H., Lee, B.R., Kim, K.H., Lee, E., Choi, J., 2015. Effects of artificial light at night on human health: A literature review of observational and experimental studies applied to exposure assessment. Chronobiology International 32, 1294–1310. URL: https://doi.org/10.3109/07420528.2015.1073158, doi:10.3109/07420528.2015.1073158. publisher: Taylor & Francis _eprint: https://doi.org/10.3109/07420528.2015.1073158.

Cordts, M., Omran, M., Ramos, S., Rehfeld, T., Enzweiler, M., Benenson, R., Franke, U., Roth, S., Schiele, B., 2016. The Cityscapes Dataset for Semantic Urban Scene Understanding. URL: http://arxiv.org/abs/1604.01685, doi:10.48550/arXiv.1604.01685. arXiv:1604.01685 [cs].

Cornish, D.B., Clarke, R.V., 2014. The reasoning criminal: Rational choice perspectives on offending. Transaction Publishers. Google-Books-ID: MPmmAgAAQBAJ.

Deng, J., Dong, W., Socher, R., Li, L.J., Li, K., Fei-Fei, L., 2009. ImageNet: A large-scale hierarchical image database, in: 2009 IEEE Conference on Computer Vision and Pattern Recognition, pp. 248–255. URL: https://ieeexplore.ieee.org/document/5206848, doi:10.1109/CVPR.2009.5206848. iSSN: 1063-6919.

Dosovitskiy, A., Beyer, L., Kolesnikov, A., Weissenborn, D., Zhai, X., Unterthiner, T., Dehghani, M., Minderer, M., Heigold, G., Gelly, S., Uszkoreit, J., Houlsby, N., 2021. An Image is Worth 16x16 Words: Transformers for Image Recognition at Scale. URL: http://arxiv.org/abs/2010.11929, doi:10.48550/arXiv.2010.11929. arXiv:2010.11929 [cs].

Duque, J.C., Lozano-Gracia, N., Patino, J.E., Restrepo, P., Velasquez, W.A., 2019. Spatiotemporal dynamics of urban growth in Latin American cities: An analysis using nighttime light imagery. Landscape and Urban Planning 191, 103640. URL: https://www.sciencedirect.com/science/article/pii/S016920461930444X, doi:10.1016/j.landurbplan.2019.103640.

Fotios, S., Gibbons, R., 2018. Road lighting research for drivers and pedestrians: The basis of luminance and illuminance recommendations. Lighting Research & Technology 50, 154–186. URL: https://doi.org/10.1177/1477153517739055, doi:10.1177/1477153517739055. publisher: SAGE Publications Ltd STM.

Goel, R., Garcia, L.M.T., Goodman, A., Johnson, R., Aldred, R., Murugesan, M., Brage, S., Bhalla, K., Woodcock, J., 2018. Estimating city-level travel patterns using street imagery: A case study of using Google Street View in Britain. PLOS ONE 13, e0196521. URL: https://journals.plos.org/plosone/article?id=10.1371/journal.pone.0196521, doi:10.1371/journal.pone.0196521. publisher: Public Library of Science.

Green, J., Perkins, C., Steinbach, R., Edwards, P., 2015. Reduced street lighting at night and health: A rapid appraisal of public views in England and Wales. Health & Place 34, 171–180. URL: https://www.sciencedirect.com/science/article/pii/S1353829215000775, doi:10.1016/j.healthplace.2015.05.011.

Guo, B., Hu, D., Liu, Y., Zheng, Q., Lin, A., Atkinson, P.M., 2024. Downscaling of nighttime light imagery with a spatially local estimation model using human activity-physical features. International Journal of Applied Earth Observation and Geoinformation 130, 103924. URL: https://www.sciencedirect.com/science/article/pii/S1569843224002784, doi:10.1016/j.jag.2024.103924.

Guo, H., Dou, C., Chen, H., Liu, J., Fu, B., Li, X., Zou, Z., Liang, D., 2023. SDGSAT-1: the world's first scientific satellite for sustainable development goals. Science Bulletin 68, 34–38. URL: https://www.sciencedirect.com/science/article/pii/S2095927322005928, doi:10.1016/j.scib.2022.12.014.

Guo, Y., Liu, Y., Oerlemans, A., Lao, S., Wu, S., Lew, M.S., 2016. Deep learning for visual understanding: A review. Neurocomputing 187, 27–48. URL: https://www.sciencedirect.com/science/article/pii/S0925231215017634, doi:10.1016/j.neucom.2015.09.116.

Hartigan, J.A., Wong, M.A., 1979. Algorithm AS 136: A K-Means Clustering Algorithm. Journal of the Royal Statistical Society. Series C (Applied Statistics) 28, 100–108. URL: https://www.jstor.org/stable/2346830, doi:10.2307/2346830. publisher: [Wiley, Royal Statistical Society].

He, K., Zhang, X., Ren, S., Sun, J., 2015. Deep Residual Learning for Image Recognition. URL: http://arxiv.org/abs/1512.03385, doi:10.48550/arXiv.1512.03385. arXiv:1512.03385 [cs].

He, K., Zhang, X., Ren, S., Sun, J., 2016. Identity Mappings in Deep Residual Networks. URL: http://arxiv.org/abs/1603.05027, doi:10.48550/arXiv.1603.05027. arXiv:1603.05027 [cs].

He, N., Li, G., 2021. Urban neighbourhood environment assessment based on street view image processing: A review of research trends. Environmental Challenges 4, 100090. URL: https://www.sciencedirect.com/science/article/pii/S266701002100069X, doi:10.1016/j.envc.2021.100090.

He, X., He, S.Y., 2023. Using open data and deep learning to explore walkability in Shenzhen, China. Transportation Research Part D: Transport and Environment 118, 103696. URL: https://www.sciencedirect.com/science/article/pii/S1361920923000937, doi:10.1016/j.trd.2023.103696.

Hee, L., Ooi, G.L., 2003. The politics of public space planning in Singapore. Planning Perspectives 18, 79–103. URL: https://doi.org/10.1080/0266543032000047413, doi:10.1080/0266543032000047413. publisher: Routledge _eprint: https://doi.org/10.1080/0266543032000047413.

Helbich, M., Browning, M.H.E.M., Huss, A., 2020. Outdoor light at night, air pollution and depressive symptoms: A cross-sectional study in the Netherlands. Science of The Total Environment 744, 140914. URL: https://www.sciencedirect.com/science/article/pii/S0048969720344430, doi:10.1016/j.scitotenv.2020.140914.

Henderson, J.V., Storeygard, A., Weil, D.N., 2012. Measuring Economic Growth from Outer Space. American Economic Review 102, 994–1028. URL: https://www.aeaweb.org/articles?id=10.1257/aer.102.2.994, doi:10.1257/aer.102.2.994.

Hou, Y., Biljecki, F., 2022. A comprehensive framework for evaluating the quality of street view imagery. International Journal of Applied Earth Observation and Geoinformation 115, 103094. URL: https://www.sciencedirect.com/science/article/pii/S1569843222002825, doi:10.1016/j.jag.2022.103094.

Hou, Y., Quintana, M., Khomiakov, M., Yap, W., Ouyang, J., Ito, K., Wang, Z., Zhao, T., Biljecki, F., 2024. Global Streetscapes — A comprehensive dataset

of 10 million street-level images across 688 cities for urban science and analytics. ISPRS Journal of Photogrammetry and Remote Sensing 215, 216–238. URL: https://www.sciencedirect.com/science/article/pii/S0924271624002612, doi:10.1016/j.isprsjprs.2024.06.023.

Hu, S., Huang, S., Hu, Q., Wang, S., Chen, Q., 2024. An commercial area extraction approach using time series nighttime light remote sensing data——Take Wuhan city as a case. Sustainable Cities and Society 100, 105032. URL: https://www.sciencedirect.com/science/article/pii/S2210670723006431, doi:10.1016/j.scs.2023.105032.

Hu, Y., Cao, X., Chen, J., 2019. Quantitative Evaluation for the Blooming Effect of Nighttime Light Data in China, in: IGARSS 2019 - 2019 IEEE International Geoscience and Remote Sensing Symposium, pp. 4312–4315. doi:10.1109/IGARSS.2019.8899107. iSSN: 2153-7003.

Ibrahim, M.R., Haworth, J., Cheng, T., 2020. Understanding cities with machine eyes: A review of deep computer vision in urban analytics. Cities 96, 102481. URL: https://www.sciencedirect.com/science/article/pii/S0264275119308443, doi:10.1016/j.cities.2019.102481.

Ignatius, M., Xu, R., Hou, Y., Liang, X., Zhao, T., Chen, S., Wong, N.H., Biljecki, F., 2022. Local Climate Zones: Lessons from Singapore and potential improvement with Street View Imagery. ISPRS Annals of the Photogrammetry, Remote Sensing and Spatial Information Sciences X-4-W2-2022, 121–128. URL: https://isprs-annals.copernicus.org/articles/X-4-W2-2022/121/2022/isprs-annals-X-4-W2-2022-121-2022.html, doi:10.5194/isprs-annals-X-4-W2-2022-121-2022. conference Name: ISPRS TC IV
17th 3D GeoInfo Conference - 19–21 October 2022, Sydney, Australia Publisher: Copernicus GmbH.

Ito, K., Biljecki, F., 2021. Assessing bikeability with street view imagery and computer vision. Transportation Research Part C: Emerging Technologies 132, 103371. URL: https://www.sciencedirect.com/science/article/pii/S0968090X21003739, doi:10.1016/j.trc.2021.103371.

Jackett, M., Frith, W., 2013. Quantifying the impact of road lighting on road safety — A New Zealand Study. IATSS Research 36, 139–145. URL: https://www.sciencedirect.com/science/article/pii/S0386111212000325, doi:10.1016/j.iatssr.2012.09.001.

Jiang, Y., Gong, X., Liu, D., Cheng, Y., Fang, C., Shen, X., Yang, J., Zhou, P., Wang, Z., 2021. EnlightenGAN: Deep Light Enhancement without Paired Supervision. URL: http://arxiv.org/abs/1906.06972. arXiv:1906.06972 [cs, eess].

Kang, Y., Zhang, F., Gao, S., Lin, H., Liu, Y., 2020. A review of urban physical environment sensing using street view imagery in public health studies. Annals of GIS 26, 261–275. URL: https://doi.org/10.1080/19475683.2020.1791954, doi:10.1080/19475683.2020.1791954. publisher: Taylor & Francis _eprint: https://doi.org/10.1080/19475683.2020.1791954.

Kaplan, J., Chalfin, A., 2022. Ambient lighting, use of outdoor spaces and perceptions of public safety: evidence from a survey experiment. Security Journal 35, 694–724. URL: https://doi.org/10.1057/s41284-021-00296-0, doi:10.1057/s41284-021-00296-0.

KartaView, 2020. Start Contributing. URL: https://kartaview.org/landing.

Ki, D., Lee, S., 2021. Analyzing the effects of Green View Index of neighborhood streets on walking time using Google Street View and deep learning. Landscape and Urban Planning 205, 103920. URL: https://www.sciencedirect.com/science/article/pii/S0169204620301018, doi:10.1016/j.landurbplan.2020.103920.

Lauko, I.G., Honts, A., Beihoff, J., Rupprecht, S., 2020. Local color and morphological image feature based vegetation identification and its application to human environment street view vegetation mapping, or how green is our county? Geo-spatial Information Science 23, 222–236. URL: https://doi.org/10.1080/10095020.2020.1805367, doi:10.1080/10095020.2020.1805367. publisher: Taylor & Francis _eprint: https://doi.org/10.1080/10095020.2020.1805367.

LeCun, Y., Bengio, Y., Hinton, G., 2015. Deep learning. Nature 521, 436–444. URL: https://www.nature.com/articles/nature14539, doi:10.1038/nature14539. number: 7553 Publisher: Nature Publishing Group.

Levin, N., Kyba, C.C.M., Zhang, Q., Sánchez de Miguel, A., Román, M.O., Li, X., Portnov, B.A., Molthan, A.L., Jechow, A., Miller, S.D., Wang, Z., Shrestha, R.M., Elvidge, C.D., 2020. Remote sensing of night lights:

A review and an outlook for the future. Remote Sensing of Environment 237, 111443. URL: https://www.sciencedirect.com/science/article/pii/S0034425719304626, doi:10.1016/j.rse.2019.111443.

Lin, Z., Jiao, W., Liu, H., Long, T., Liu, Y., Wei, S., He, G., Portnov, B.A., Trop, T., Liu, M., Li, X., Wen, C., 2023. Modelling the Public Perception of Urban Public Space Lighting Based on SDGSAT-1 Glimmer Imagery: A Case Study in Beijing, China. Sustainable Cities and Society 88, 104272. URL: https://www.sciencedirect.com/science/article/pii/S2210670722005777, doi:10.1016/j.scs.2022.104272.

Lis, A., Zienowicz, M., Kukowska, D., Zalewska, K., Iwankowski, P., Shestak, V., 2023. How to light up the night? The impact of city park lighting on visitors' sense of safety and preferences. Urban Forestry & Urban Greening 89, 128124. URL: https://www.sciencedirect.com/science/article/pii/S1618866723002959, doi:10.1016/j.ufug.2023.128124.

Liu, H., Wan, Z., Huang, W., Song, Y., Han, X., Liao, J., 2021. PD-GAN: Probabilistic Diverse GAN for Image Inpainting, pp. 9371–9381. URL: https://openaccess.thecvf.com/content/CVPR2021/html/Liu_PD-GAN_Probabilistic_Diverse_GAN_for_Image_Inpainting_CVPR_2021_paper.html.

Liu, Z., Li, T., Ren, T., Chen, D., Li, W., Qiu, W., 2024. Day-to-Night Street View Image Generation for 24-Hour Urban Scene Auditing Using Generative AI. Journal of Imaging 10, 112. URL: https://www.ncbi.nlm.nih.gov/pmc/articles/PMC11121941/, doi:10.3390/jimaging10050112.

Lunn, R.M., Blask, D.E., Coogan, A.N., Figueiro, M.G., Gorman, M.R., Hall, J.E., Hansen, J., Nelson, R.J., Panda, S., Smolensky, M.H., Stevens, R.G., Turek, F.W., Vermeulen, R., Carreón, T., Caruso, C.C., Lawson, C.C., Thayer, K.A., Twery, M.J., Ewens, A.D., Garner, S.C., Schwingl, P.J., Boyd, W.A., 2017. Health consequences of electric lighting practices in the modern world: A report on the National Toxicology Program's workshop on shift work at night, artificial light at night, and circadian disruption. Science of The Total Environment 607-608, 1073–1084. URL: https://www.sciencedirect.com/science/article/pii/S004896971731759X, doi:10.1016/j.scitotenv.2017.07.056.

Mellander, C., Lobo, J., Stolarick, K., Matheson, Z., 2015. Night-Time Light Data: A Good Proxy Measure for Economic Activity? PLOS ONE 10, e0139779. URL: https://journals.plos.org/plosone/article?id=10.1371/journal.pone.0139779, doi:10.1371/journal.pone.0139779. publisher: Public Library of Science.

NASA, 2021. Nighttime Lights. URL: https://www.earthdata.nasa.gov/learn/backgrounders/nighttime-lights. publisher: Earth Science Data Systems, NASA.

Ning, H., Li, Z., Ye, X., Wang, S., Wang, W., Huang, X., 2022. Exploring the vertical dimension of street view image based on deep learning: a case study on lowest floor elevation estimation. International Journal of Geographical Information Science 36, 1317–1342. URL: https://doi.org/10.1080/13658816.2021.1981334, doi:10.1080/13658816.2021.1981334. publisher: Taylor & Francis _eprint: https://doi.org/10.1080/13658816.2021.1981334.

Ntarara, E., Syngkiridi, K., Androvitsaneas, V.P., Doulos, L.T., 2022. The impact of lighting trespass on nearby buildings and their inhabitants which derives from municipal stadiums. Early results from a post occupancy evaluation survey. IOP Conference Series: Earth and Environmental Science 1123, 012034. URL: https://dx.doi.org/10.1088/1755-1315/1123/1/012034, doi:10.1088/1755-1315/1123/1/012034. publisher: IOP Publishing.

Painter, K., Farrington, D.P., 1999. Street Lighting And Crime: Diffusion Of Benefits In The Stoke-on-trent Project. Crime Prevention Studies volume 10, 77–122.

Pan, W., Du, J., 2021. Impacts of urban morphological characteristics on nocturnal outdoor lighting environment in cities: An empirical investigation in Shenzhen. Building and Environment 192, 107587. URL: https://www.sciencedirect.com/science/article/pii/S0360132321000032, doi:10.1016/j.buildenv.2021.107587.

Pang, H.E., Biljecki, F., 2022. 3D building reconstruction from single street view images using deep learning. International Journal of Applied Earth Observation and Geoinformation 112, 102859. URL: https://

www.sciencedirect.com/science/article/pii/S1569843222000619, doi:10.1016/j.jag.2022.102859.

Rahm, J., Sternudd, C., Johansson, M., 2021. "In the evening, I don't walk in the park": The interplay between street lighting and greenery in perceived safety. URBAN DESIGN International 26, 42–52. URL: https://doi.org/10.1057/s41289-020-00134-6, doi:10.1057/s41289-020-00134-6.

Ritonja, J., McIsaac, M.A., Sanders, E., Kyba, C.C.M., Grundy, A., Cordina-Duverger, E., Spinelli, J.J., Aronson, K.J., 2020. Outdoor light at night at residences and breast cancer risk in Canada. European Journal of Epidemiology 35, 579–589. URL: https://doi.org/10.1007/s10654-020-00610-x, doi:10.1007/s10654-020-00610-x.

Rousseeuw, P.J., 1987. Silhouettes: A graphical aid to the interpretation and validation of cluster analysis. Journal of Computational and Applied Mathematics 20, 53–65. URL: https://www.sciencedirect.com/science/article/pii/0377042787901257, doi:10.1016/0377-0427(87)90125-7.

Sharifi Noorian, S., Qiu, S., Psyllidis, A., Bozzon, A., Houben, G.J., 2020. Detecting, Classifying, and Mapping Retail Storefronts Using Street-level Imagery, in: Proceedings of the 2020 International Conference on Multimedia Retrieval, Association for Computing Machinery, New York, NY, USA. pp. 495–501. URL: https://dl.acm.org/doi/10.1145/3372278.3390706, doi:10.1145/3372278.3390706.

Shi, L., Wurm, M., Huang, X., Zhong, T., Leichtle, T., Taubenböck, H., 2020. Urbanization that hides in the dark – Spotting China's "ghost neighborhoods" from space. Landscape and Urban Planning 200, 103822. URL: https://www.sciencedirect.com/science/article/pii/S0169204619314185, doi:10.1016/j.landurbplan.2020.103822.

Shi, Z., Zhu, M.m., Guo, B., Zhao, M., Zhang, C., 2018. Nighttime low illumination image enhancement with single image using bright/dark channel prior. EURASIP Journal on Image and Video Processing 2018, 13. URL: https://doi.org/10.1186/s13640-018-0251-4, doi:10.1186/s13640-018-0251-4.

Sim, L.L., Yu, S.M., Malone-Lee, L.C., 2002. Re-Examining the Retail Hierarchy in Singapore: Are the Town Centres and Neighbourhood Centres Sustain-

able? The Town Planning Review 73, 63–81. URL: https://www.jstor.org/stable/40112483. publisher: Liverpool University Press.

Simonyan, K., Zisserman, A., 2015. Very Deep Convolutional Networks for Large-Scale Image Recognition. URL: http://arxiv.org/abs/1409.1556, doi:10.48550/arXiv.1409.1556. arXiv:1409.1556 [cs].

Sung, C.Y., 2022. Examining the effects of vertical outdoor built environment characteristics on indoor light pollution. Building and Environment 210, 108724. URL: https://www.sciencedirect.com/science/article/pii/S0360132321011148, doi:10.1016/j.buildenv.2021.108724.

Tan, M., Le, Q.V., 2020. EfficientNet: Rethinking Model Scaling for Convolutional Neural Networks. URL: http://arxiv.org/abs/1905.11946, doi:10.48550/arXiv.1905.11946. arXiv:1905.11946 [cs, stat].

Tong, J.C.K., Wun, A.H.L., Chan, T.T.H., Lau, E.S.L., Lau, E.C.F., Chu, H.H.K., Lau, A.P.S., 2023. Simulation of vertical dispersion and pollution impact of artificial light at night in urban environment. Science of The Total Environment 902, 166101. URL: https://www.sciencedirect.com/science/article/pii/S0048969723047265, doi:10.1016/j.scitotenv.2023.166101.

Torii, A., Arandjelović, R., Sivic, J., Okutomi, M., Pajdla, T., 2015. 24/7 place recognition by view synthesis, in: 2015 IEEE Conference on Computer Vision and Pattern Recognition (CVPR), pp. 1808–1817. doi:10.1109/CVPR.2015.7298790. iSSN: 1063-6919.

Vallée, A., Lecarpentier, Y., Guillevin, R., Vallée, J.N., 2020. The influence of circadian rhythms and aerobic glycolysis in autism spectrum disorder. Translational Psychiatry 10, 1–10. URL: https://www.nature.com/articles/s41398-020-01086-9, doi:10.1038/s41398-020-01086-9. publisher: Nature Publishing Group.

Walker, F.W., Roberts, S.E., 1976. Influence of lighting on accident frequency at highway intersections. Transportation research record 562, 73–78. URL: https://www.safetylit.org/citations/index.php?fuseaction=citations.viewdetails&citationIds[]=citjournalarticle_483461_38.

Wang, J., Biljecki, F., 2022. Unsupervised machine learning in urban studies: A systematic review of applications. Cities 129, 103925. URL: https://www.sciencedirect.com/science/article/pii/S026427512200364X, doi:10.1016/j.cities.2022.103925.

Wang, J., Lu, F., 2021. Modeling the electricity consumption by combining land use types and landscape patterns with nighttime light imagery. Energy 234, 121305. URL: https://www.sciencedirect.com/science/article/pii/S036054422101553X, doi:10.1016/j.energy.2021.121305.

Wang, L., Fan, H., Wang, Y., 2020. Improving population mapping using Luojia 1-01 nighttime light image and location-based social media data. Science of The Total Environment 730, 139148. URL: https://www.sciencedirect.com/science/article/pii/S0048969720326656, doi:10.1016/j.scitotenv.2020.139148.

Wang, T., Kaida, N., Kaida, K., 2023. Effects of outdoor artificial light at night on human health and behavior: A literature review. Environmental Pollution 323, 121321. URL: https://www.sciencedirect.com/science/article/pii/S0269749123003238, doi:10.1016/j.envpol.2023.121321.

Wang, T., Sun, F., 2022. Global gridded GDP data set consistent with the shared socioeconomic pathways. Scientific Data 9, 221. URL: https://www.nature.com/articles/s41597-022-01300-x, doi:10.1038/s41597-022-01300-x. number: 1 Publisher: Nature Publishing Group.

Wanvik, P.O., 2009. Effects of road lighting: An analysis based on Dutch accident statistics 1987–2006. Accident Analysis & Prevention 41, 123–128. URL: https://www.sciencedirect.com/science/article/pii/S0001457508001917, doi:10.1016/j.aap.2008.10.003.

Welsh, B.C., Farrington, D.P., Douglas, S., 2022. The impact and policy relevance of street lighting for crime prevention: A systematic review based on a half-century of evaluation research. Criminology & Public Policy 21, 739–765. URL: https://onlinelibrary.wiley.com/doi/abs/10.1111/1745-9133.12585, doi:10.1111/1745-9133.12585. _eprint: https://onlinelibrary.wiley.com/doi/pdf/10.1111/1745-9133.12585.

Wold, S., Esbensen, K., Geladi, P., 1987. Principal component analysis. Chemometrics and Intelligent Laboratory Systems 2, 37–52. URL: https://www.sciencedirect.com/science/article/pii/0169743987800849, doi:10.1016/0169-7439(87)80084-9.

Woo, A., Han, J., Shin, H., Lee, S., 2024. Economic benefits of urban streetscapes: Analyzing the interrelationships between visual street environments and single-family property values in Seoul, Korea. Applied Geography 163, 103182. URL: https://www.sciencedirect.com/science/article/pii/S0143622823003132, doi:10.1016/j.apgeog.2023.103182.

Xiao, Q., Gee, G., Jones, R.R., Jia, P., James, P., Hale, L., 2020. Cross-sectional association between outdoor artificial light at night and sleep duration in middle-to-older aged adults: The NIH-AARP Diet and Health Study. Environmental Research 180, 108823. URL: https://www.sciencedirect.com/science/article/pii/S0013935119306206, doi:10.1016/j.envres.2019.108823.

Xie, Y., Weng, Q., 2016. World energy consumption pattern as revealed by DMSP-OLS nighttime light imagery. GIScience & Remote Sensing 53, 265–282. URL: https://doi.org/10.1080/15481603.2015.1124488, doi:10.1080/15481603.2015.1124488. publisher: Taylor & Francis _eprint: https://doi.org/10.1080/15481603.2015.1124488.

Xu, G., Xiu, T., Li, X., Liang, X., Jiao, L., 2021. Lockdown induced night-time light dynamics during the COVID-19 epidemic in global megacities. International Journal of Applied Earth Observation and Geoinformation 102, 102421. URL: https://www.sciencedirect.com/science/article/pii/S0303243421001288, doi:10.1016/j.jag.2021.102421.

Xu, Y., Fu, C., Kennedy, E., Jiang, S., Owusu-Agyemang, S., 2018. The impact of street lights on spatial-temporal patterns of crime in Detroit, Michigan. Cities 79, 45–52. URL: https://www.sciencedirect.com/science/article/pii/S0264275117311368, doi:10.1016/j.cities.2018.02.021.

Yang, Y., Ma, M., Zhu, X., Ge, W., 2020. Research on spatial characteristics of metropolis development using nighttime light data: NTL based spatial characteristics of Beijing. PLOS ONE 15, e0242663. URL: https://journals.plos.org/plosone/article?id=10.1371/journal.pone.0242663, doi:10.1371/journal.pone.0242663. publisher: Public Library of Science.

Yannis, G., Kondyli, A., Mitzalis, N., 2013. Effect of lighting on frequency and severity of road accidents. Proceedings of the Institution of Civil Engineers - Transport 166, 271–281. URL: https://www.icevirtuallibrary.com/doi/abs/10.1680/tran.11.00047, doi:10.1680/tran.11.00047. publisher: ICE Publishing.

Yin, G., Liu, Y., Chen, Y., 2024. "Ghost city" or habitable city? The production and transformation of space in China's new towns. Cities 145, 104678. URL: https://www.sciencedirect.com/science/article/pii/S0264275123004900, doi:10.1016/j.cities.2023.104678.

Yu, B., Lian, T., Huang, Y., Yao, S., Ye, X., Chen, Z., Yang, C., Wu, J., 2019. Integration of nighttime light remote sensing images and taxi GPS tracking data for population surface enhancement. International Journal of Geographical Information Science 33, 687–706. URL: https://doi.org/10.1080/13658816.2018.1555642, doi:10.1080/13658816.2018.1555642. publisher: Taylor & Francis _eprint: https://doi.org/10.1080/13658816.2018.1555642.

Yu, F., Chen, H., Wang, X., Xian, W., Chen, Y., Liu, F., Madhavan, V., Darrell, T., 2020. BDD100K: A Diverse Driving Dataset for Heterogeneous Multitask Learning. URL: http://arxiv.org/abs/1805.04687, doi:10.48550/arXiv.1805.04687. arXiv:1805.04687 [cs].

Zhang, A., Li, W., Wu, J., Lin, J., Chu, J., Xia, C., 2021. How can the urban landscape affect urban vitality at the street block level? A case study of 15 metropolises in China. Environment and Planning B: Urban Analytics and City Science 48, 1245–1262. URL: https://doi.org/10.1177/2399808320924425, doi:10.1177/2399808320924425. publisher: SAGE Publications Ltd STM.

Zhang, F., Salazar-Miranda, A., Duarte, F., Vale, L., Hack, G., Liu, Y., Batty, M., Ratti, C., 2023a. Urban Visual Intelligence: Studying Cities with AI and Street-level Imagery URL: https://arxiv.org/abs/2301.00580, doi:10.48550/ARXIV.2301.00580. publisher: arXiv Version Number: 1.

Zhang, F., Wu, L., Zhu, D., Liu, Y., 2019. Social sensing from street-level imagery: A case study in learning spatio-temporal urban mobility patterns. ISPRS Journal of Photogrammetry and Remote Sensing 153, 48–58. URL: https://www.sciencedirect.com/science/article/pii/S0924271619301133, doi:10.1016/j.isprsjprs.2019.04.017.

Zhang, J., Liu, X., Tan, X., Jia, T., Senousi, A.M., Huang, J., Yin, L., Zhang, F., 2022. Nighttime Vitality and Its Relationship to Urban Diversity: An Exploratory Analysis in Shenzhen, China. IEEE Journal of Selected Topics in Applied Earth Observations and Remote Sensing 15, 309–322. doi:10.1109/JSTARS.2021.3130763. conference Name: IEEE Journal of Selected Topics in Applied Earth Observations and Remote Sensing.

Zhang, X., Li, P., 2018. A temperature and vegetation adjusted NTL urban index for urban area mapping and analysis. ISPRS Journal of Photogrammetry and Remote Sensing 135, 93–111. URL: https://www.sciencedirect.com/science/article/pii/S0924271617303611, doi:10.1016/j.isprsjprs.2017.11.016.

Zhang, Y., Liu, P., Biljecki, F., 2023b. Knowledge and topology: A two layer spatially dependent graph neural networks to identify urban functions with time-series street view image. ISPRS Journal of Photogrammetry and Remote Sensing 198, 153–168. URL: https://www.sciencedirect.com/science/article/pii/S0924271623000680, doi:10.1016/j.isprsjprs.2023.03.008.

Zhang, Y., Song, S., Li, X., Gao, S., Raubal, M., 2024. Leveraging context-adjusted nighttime light data for socioeconomic explanations of global urban resilience. Sustainable Cities and Society 114, 105739. URL: https://www.sciencedirect.com/science/article/pii/S221067072400564X, doi:10.1016/j.scs.2024.105739.

Zhao, M., Zhou, Y., Li, X., Cao, W., He, C., Yu, B., Li, X., Elvidge, C.D., Cheng, W., Zhou, C., 2019. Applications of Satellite Remote Sensing of Nighttime Light Observations: Advances, Challenges, and Perspectives. Remote Sensing 11, 1971. URL: https://www.mdpi.com/2072-4292/11/17/1971, doi:10.3390/rs11171971. number: 17 Publisher: Multidisciplinary Digital Publishing Institute.

Zhao, N., Cao, G., Zhang, W., Samson, E.L., 2018. Tweets or nighttime lights: Comparison for preeminence in estimating socioeconomic factors. ISPRS Journal of Photogrammetry and Remote Sensing 146, 1–10. URL: https://www.sciencedirect.com/science/article/pii/S0924271618302375, doi:10.1016/j.isprsjprs.2018.08.018.

Zhao, T., Liang, X., Tu, W., Huang, Z., Biljecki, F., 2023. Sensing urban soundscapes from street view imagery. Computers, Environment and Urban Systems 99, 101915. URL: https://www.sciencedirect.com/science/article/pii/S0198971522001594, doi:10.1016/j.compenvurbsys.2022.101915.

Zheng, Q., Seto, K.C., Zhou, Y., You, S., Weng, Q., 2023. Nighttime light remote sensing for urban applications: Progress, challenges, and prospects. ISPRS Journal of Photogrammetry and Remote Sensing 202, 125–141. URL: https://www.sciencedirect.com/science/article/pii/S0924271623001521, doi:10.1016/j.isprsjprs.2023.05.028.

Zhou, B., Zhao, H., Puig, X., Xiao, T., Fidler, S., Barriuso, A., Torralba, A., 2019. Semantic Understanding of Scenes Through the ADE20K Dataset. International Journal of Computer Vision 127, 302–321. URL: https://doi.org/10.1007/s11263-018-1140-0, doi:10.1007/s11263-018-1140-0.

Zhu, J.Y., Park, T., Isola, P., Efros, A.A., 2020. Unpaired image-to-image translation using cycle-consistent adversarial networks. URL: http://arxiv.org/abs/1703.10593, doi:10.48550/arXiv.1703.10593. arXiv:1703.10593 [cs].

Zielinska-Dabkowska, K.M., Schernhammer, E.S., Hanifin, J.P., Brainard, G.C., 2023. Reducing nighttime light exposure in the urban environment to benefit human health and society. Science 380, 1130–1135. URL: https://www.science.org/doi/full/10.1126/science.adg5277, doi:10.1126/science.adg5277. publisher: American Association for the Advancement of Science.